Model Based Snow Cover Analysis Regarding the Avalanches in Longyearbyen 2015 and 2017

Magnus Myhre

Master's Thesis in Geoscience
Discipline: Geohazards
30 Credits

Department of Geosciences
Faculty of Mathematics and Natural Sciences

UNIVERSITY OF OSLO

June 2018

Master's Thesis, Department of Geosciences

Model Based Snow Cover Analysis Regarding the Avalanches in Longyearbyen 2015 and 2017

Magnus Myhre

Title: Model Based Snow Cover Analysis Regarding the Avalanches in Longyearbyen 2015 and 2017

Author: Magnus Myhre

Guidance Chancellors: Thomas Schuler (UIO) and Karsten Müller (NVE)

Cover photo: © LOYALTYLOBBY

http://www.duo.uio.no/

Print: Reprosentralen, University of Oslo

Abstract

Traditionally, avalanche danger assessment and forecasting requires a professional to physically sample crucial data in the field. The primary weakness of this method concerns sparse observations in space and time. CROCUS is a numerical snow cover model capable of bypassing both disadvantages as it provides continuous updates on the conditions, in addition to its ability to simulate a myriad of locations simultaneously, with meteorological input data as the only requirement. Because snowpack evolution differentiates in different regions and the model primarily are tested in the French Alps, this study works to assess the snow cover model CROCUS' performance with forcing from AROME-Arctic in a region yet untested, namely Longyearbyen, Svalbard. To appropriately conduct this assessment two past avalanche events were revisited in the light of the models performance. Specifically the destructive events that transpired 19.12.15 and 21.02.17, where no forecasters managed to anticipate the substantial hazard. In that regard, three research questions were addressed: (1) Evaluate the models ability to reproduce the observed snowpack stratigraphy, and furthermore indicate avalanche danger at the correct time step in Longyearbyen. (2) Investigate whether forcing data from AROME-Arctic provides suitable input to the model, when aiming to forecast avalanche danger in Longyearbyen. (3) Investigate how future forecasters can use snowpack simulations to support stability assessments in Longyearbyen.

Firstly, the study found that CROCUS simulates snowpacks very similar to those observed in the field, provided satisfactory simulations of snowpack thickness, independent of the forcing being artificial or natural. Secondly, an analysis of the model approach to forcing in comparison to its counterpart of automatic weather stations found that AROME-Arctic were superior regarding spatial density, operativeness and ability to forecast. AROME-Arctic is therefore suitable as forcing for CROCUS from the perspective of avalanche danger forecasting the region. Finally, regarding the models future applications, the study found that because of the uncertainties regarding the models ability to reproduce snowpack thickness, and the absence of destructive testing in the model workflow, a complete dependence on the models capability is premature. However, due to the superior time and spatial density of the model, in comparison with traditional methods it can very much supplement the current methods. Therefore, a hybrid approach has the potential to be beneficial in the future, regarding utilizing CROCUS as an avalanche danger forecasting tool in Longyearbyen.

Acknowledgements

Working with this thesis has been a deeply interesting, but challenging endeavor. In that regard some acknowledgements are in its place. Firstly, my family undoubtedly deserves some gratitude. Considering the social input my brother provided me with every day I worked from home at exactly 1500, and my family's sincere support throughout the duration of these five years. This product, and token of my academic achievements would never have been possible.

Furthermore, a thanks to my fellow students. Providing good humor, and most important, a sense of affiliation in this period have been crucial working with this thesis. In addition, a special thanks to my girlfriend, Sandra. Working wonders with my circadian rhythm and listening to me rant about the content of this paper for five consecutive months. Giving me motivation to put in some extra work. Also, all of my friends outside of school and the remainder of my closest social circle deserve some appreciation. Giving me the strength and necessary grit to sustain and complete my studies within the regular time frame.

Finally, a word to my primary guidance chancellor, Thomas Schuler: Your substantive feedback, keeping me on track and away from misinterpretations and other pitfalls have been essential, providing this thesis with additional purpose.

You have all been invaluable to my progress and journey, reaching this result. In which I have grown very proud off.

Magnus Myhre — Oslo, 14.06.18

Table of Contents

1 Introduction

Avalanche danger assessment and forecasting can be a challenging, demanding and dangerous affair. Traditionally, a synopsis of all major, quantifiable avalanche factors at many representative locations in a region allows an approximation of the prevailing degree of stability in a region (Buser, Föhn, Good, Gubler, & Salm, 1985). This process however, requires a professional to physically sample crucial data in the field, which potentially is a physically exhausting, and dangerous endeavor as it might involve entering an already unstable location. Although, when this process is concluded, the acquisition of data only represents one point in space and time, which is insufficient when assessing avalanche danger in a broader region (Temper, 2008). Therefore, a majority of data points have to be sited where safe access is guaranteed in wintertime. Consequently, representativeness is compromised, despite being of upmost importance (Buser, Föhn, Good, Gubler, & Salm, 1985). Another disadvantage concerning the traditional method of assessment and forecasting is the lack of information in between observations. Which makes some effects such as snow-crystal growth with varying surface temperature and radiation penetration extremely difficult to forecast with in situ observations as the source of data (Brun, David, Sudul, & Brunot, 1992). CROCUS is a numerical snow cover model capable of bypassing both disadvantages as it provides continuous updates on the snowpack conditions, in addition to its ability to simulate a myriad of locations simultaneously, where meteorological input data is the only requirement needed (Vionnet, et al., 2012). Including such a model in the avalanche forecasting routine in any area seem unavoidable, due to the models capability to provide the same information as traditional methods, excluded destructive testing. In addition to providing information with greater frequency and spatial density, a model approach will remove the danger element from the traditional assessment process. Which is of pivotal interest when aiming to increase the quality, accuracy and safety of avalanche danger assessment and forecasting in a region.

The model however, is primarily validated in the French Alps, with satisfactory results reflected in the models immense accuracy (Brun, Martin, Simon, Gendre, & Coleou, 1989: Brun, David, Sudul, & Brunot, 1992). This provides a demand. Because the evolution of a snowpack is controlled by the prevailing meteorological conditions (Durand, Giraud, Brun, Mérindol , & Martin, 1999), it will consequently differentiate from one region to another. Therefore, the model cannot be introduced as a tool for avalanche danger forecasting to an arbitrary region without intricate testing beforehand. With that in mind, this thesis will work to assess the snow cover model CROCUS' performance with forcing from AROME-Arctic in a region yet untested, namely Longyearbyen, Svalbard. Here, frequent avalanches threaten infrastructure and general human safety throughout the winter season (Eckerstorfer & Christiansen, 2011), resulting in a necessity to continuously increase the quality and accuracy of the avalanche forecasting process. Of which CROCUS potentially can be an essential enhancement.

1.1 General Note on Crocus

Concerning the context of using a numerical snow cover model to simulate the prevailing conditions in a region, a note on CROCUS in general and its definition is beneficial. Considering earlier validations of the model, expected limitations and under what assumptions CROCUS can be utilized to assess avalanche danger.

CROCUS is a one-dimensional multilayer physical snow scheme. It simulates the evolution of the snow cover as a function of energy and mass-transfer between the snowpack and the atmosphere. The time and space evolution of the snowpack is key to many scientific and socio-economic applications, such as weather, hydrological, and in the case of this thesis, avalanche risk forecasting (Vionnet, et al., 2012). Local validations of the model however, were from Brun, David, Sudul and Brunot (1992) at Col de Porte, France. Here, all meteorological parameters was measured and recorded. Then, this forcing provided CROCUS with the required prerequisites to simulate the evolution of the internal state of the snow cover, which was compared with observations collected weakly from a snowpit at the site. During this test, CROCUS simulated snowpacks very similar to those observed in the field.

In Norway, previous attempts utilizing and assessing CROCUS within SURFEX have in one instance been performed by Vikhamar-Schuler, Müller and Engen-Skaugen (2011). Here, they aimed to model the snowpack stratigraphy at locations of weather stations, evaluating the results with available snowpit measurements. They found that the model satisfactory simulated snow depth and other variables. However, when assessing different forms of forcing data they found that the models estimations of snow depth are the most sensitive to precipitation and temperature input. And least sensitive to air humidity, surface air pressure and wind speeds (Vikhamar-Schuler, Müller, & Engen-Skaugen, 2011). Such an assessment confirms the models sensitivity to external factors, such as forcing. Consequently leading to the necessity of evaluating the chosen forcing in the interest of assessing the model. Furthermore, in addition to these results they concluded that modeling of snow profiles in Norway are especially interesting due to the low density network of field observations and automatic weather stations (IBID). Further justifying the purpose of this thesis.

When Durand, Giraud, Brun, Mérindol and Martin (1999) assessed the model, they found some significant drawbacks concerning the use of this model in general. The most fundamental weakness of running this system is that there is a cumulative effect of all the daily errors throughout the season with no direct correction possible. In addition, they found another weakness, concerning the models inability to simulate accumulation by wind, which may significantly modify the local snow conditions. At Svalbard, redistribution by wind play a major role distributing the snow, whereas some patches might be completely free of snow, and others might be covered in several meters (Eckerstorfer, 2013). In that regard, a hypothesis on the models performance will be proposed based on these limitations: The snow cover model CROCUS are expected to underestimate the snowpack thickness, because it does not take redistribution by wind into account. A consequence of such an implication is a possible quantification of the models sensitivity to internal factors, like program workflow. Therefore, it is pivotal to address this issue, if it occurs.

On a more specific note, adopting CROCUS as a tool for avalanche danger forecasting can potentially cause challenges. A fundamental one of which concerns local snowpack stratigraphy differentiating considerably within a region. This variable is strongly influenced by microtopography, especially wind drift, which is capable of producing great spatial variability. However, avalanche danger forecasting is possible at a larger scale, because the snowpack of a given region present similar features at similar elevations on slopes of similar aspect. This is particularly the case for the presence of weak layers and the occurrence of processes like melting and refreezing. Since the evolution of a snowpack is controlled by the prevailing local meteorological conditions, the following assumption can be made: it is possible, for a set of elevations and aspects to simulate the evolution of the main characteristics of the snowpack in a given region from the average meteorological conditions prevailing in that region (Durand, Giraud, Brun, Mérindol , & Martin, 1999). Under this assumption, it is possible to forecast avalanche danger in a broader region based on the main characteristics of several, simulated snowpacks.

However, weaknesses, limitations, sensitivities and negative hypothesis considered, the expectations to the model in general are confident. Considering CROCUS has been run operationally for avalanche danger forecasting in the French mountains for approximately quarter of a century (Vionnet, et al., 2012). This is pivotal, because it establishes the ethos of the model, and indicates general consensus regarding the models performance.

1.2 Scope of Thesis and Research Question

This study will work to assess the numerical snow cover model CROCUS' performance outside of its origin, specifically, Longyearbyen, Svalbard. For this to be executed appropriately two past avalanche events will be revisited in the light of the models performance. Specifically, the destructive events that transpired 19.12.15 and 21.02.17, where no forecasters managed to anticipate the substantial, prevailing hazard (DSB, 2016: Landrø, Mikkelsen & Jaedicke, 2017). In general, CROCUS will be utilized to simulate the conditions in the relevant area based on the already registered weather forecasts from AROME-Arctic. These results will further be interpreted to assess whether the model system is able to reproduce the observed snowpack stratigraphy and furthermore indicate avalanche danger at the correct time step. In addition, because the models performance is dependent on the forcing, consequently generating insecurities (Vikhamar-Schuler, Müller, & Engen-Skaugen, 2011), an assessment of whether AROME-Arctic provides satisfactory input is imminent. However, this combined assessment of the model systems performance with this specific input provides the foundation to an assessment of whether this composition is suitable to support future avalanche forecasters stability assessments, in this region.

Therefore, in this thesis, the following research questions will be addressed:

- Assessing the snow cover model CROCUS' performance within the framework proposed.
  - Evaluate the models ability to reproduce the observed snowpack stratigraphy, and furthermore indicate avalanche danger at the correct time step in Longyearbyen.
  - Investigate whether forcing data from AROME-Arctic provides suitable input to the model, when aiming to forecast avalanche danger in Longyearbyen.
  - Investigate how future forecasters can use snowpack simulations to support stability assessments in Longyearbyen.

1.3 Study Area

The area in question concerning this thesis is Longyearbyen, the main settlement in Svalbard. Longyearbyen is located at 78° 13'N, 15° 47'E, in the center of Svalbards main island, Spitsbergen. (Eckerstorfer, 2013) (Fig. 1). Specifically, Longyearbyen is located in the valley Longyeardalen, a typical glaciofluvially eroded U-shaped valley, deglaciated around 10 000 BP (Svendsen & Mangerud, 1997). The location of the destructive events is Sukkertoppen (DSB, 2016: Landrø, Mikkelsen, & Jaedicke, 2017) (Fig. 2), which rises 371 m a.s.l. and are located at the eastside of the entrance to Longyeardalen (Bolstad & Barr, 2017). Furthermore, the landscape around Longyearbyen lies in the Central Tertiary Basin, consisting of horizontal-lying, sedimentary bedrock of Early Permian to Eocene age (Major, Haremo, Dallmann, & Andresen, 2001). This geological setting determines the extensive plateau mountain topography rising to an average elevation of 450 – 500 m a.s.l. (Eckerstorfer, 2013).

Weather in the Arctic is characterized by an alternating pattern of high and low pressure systems reflected in seasonal and daily air temperature fluctuations in Longyearbyen (Schaerer, 1986). During the winter season, which is the most relevant time period for this thesis, meridional moisture transport along the North Atlantic cyclone track brings warm air temperatures and precipitation to Svalbard (Dickson, et al., 2000). From the north, cold anticyclonic air masses change with these moist cyclonic air masses resulting in large air temperature variations during the winter (Humlum, Christiansen, & Juliussen, 2007).

Furthermore, the extent of large-scale phenomena such as the Siberian High, an intense, cold anticyclone, influences especially winter air temperature conditions (Humlum, Instanes, & Sollid, 2003). When the Siberian High extends to the west, covering parts of Europe, airflow over the Nordic Sea is strong and southerly, causing advection of warm air to the Svalbard region. Conversely, when cold polar air masses extend over Svalbard, a strong westerly airflow blows over northern Europe, creating heavy precipitation (Humlum, Instanes, & Sollid, 2003). The climate sensibility is also enhanced by rapid variations in the sea ice extent that is coupled with both atmospheric and oceanic circulations (Humlum, 2002). The area of the Svalbard Archipelago is recognized as one of the most climatically sensitive in the world (Rogers, Yang, & Li, 2005).

Locally, wind is constantly blowing. Due to its consistency and strength and the lack of any high vegetation, winds significantly redistribute snow in the landscape. Some parts are complete free of snow for most of the winter, while in lee sides, snow accumulates up to several meters thick. The prevailing winter wind direction over central Svalbard is the SE, while local wind directions may vary due to topographical channeling effects (Eckerstorfer, 2013).

Figure 1: General study area, location of Longyearbyen, Svalbard (Eckerstorfer, 2013)

Figure 2: Approximate outline of destructive events in Longyearbyen (Norgeskart, 2018)

1.4 Review of Events

The events in interest concerning this thesis are the destructive avalanches that transpired 19.12.15 (DSB, 2016) and 21.02.17 (Landrø, Mikkelsen, & Jaedicke, 2017), both affecting the same area in Longyearbyen (Fig. 2). The following subsection provides a short description of the two events, regarding which preconditions consequently led to the events, and how they transpired in general.

1.4.1 2015 Event

19.12.15 a major avalanche were triggered from Sukkertoppen in Longyearbyen at 10:23 in the morning. The resultant slab contained a volume of approximately 20 000 m^3 (or 5 000 tons), whereas the fracture line ranged from 2 – 3 meters in height and measured 200 meters in length. Consequently, the avalanche collided with the settlement downhill causing the houses closest to the slope to loosen from their foundations and further being moved in the same trajectory as the avalanche until they collided with the succeeding line of houses (Fig. 3). A total of eleven houses were physically moved and completely destroyed during the event. Even though two of the houses were empty, twenty-five people were present in the remaining nine houses. Whereas two of those people tragically passed away (DSB, 2016).

Figure 3: Aerial photo showing the extent of the 2015 event (DSB, 2016)

The preconditions leading up to the event were divers. The temperatures fluctuated between a minimum of -17.2 °C at 16.12 (Yr, 2015a) and maximum temperatures close to 0 °C approaching the event (Yr, 2015b). In addition to wind speeds reaching 28.9 m/s during the night leading up to the event (Yr, 2015c). Even though the wind and temperature measurements reached extreme values, this is not true regarding the measurements of freshly fallen snow. Estimating amounts of fallen snow under such conditions however, is extremely difficult. Because the extreme wind speeds causes tremendous redistribution of already settled snow. Regardless of the existence of satisfactory estimations, the qualitative impression of the inhabitants was that they woke up on 19.12 to unusual amounts of snow. To the degree where some had to climb out windows to get outside, in addition to most roads being impassable (DSB, 2016).

Furthermore, the DSB report following the event concluded that the low temperatures prior to the event, combined with a thin snow cover caused a weak layer to be formed and later buried during the storm. Increased temperatures caused the newly settled snow to increase in density and further increase the force applied to the weak layer. The corresponding weight to the wind transported snow caused the weak layer formed during the cold period to collapse and the slab to propagate (DSB, 2016).

1.4.2 2017 Event

21.02.17 two avalanches were triggered from Sukkertoppen in Longyearbyen, one of which hit three buildings (Fig 4). Even though two of the buildings hosted residents, there were not reported any injuries. The ultimately destructive avalanche consisted of two events. First, a primary avalanche was triggered at 300 m a.s.l., which was partly deposited at 235 m a.s.l..

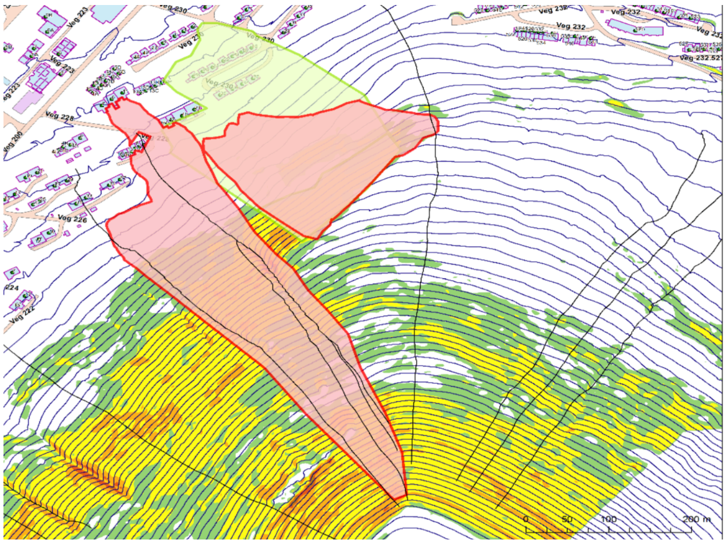

Figure 4: Extent of 2017 event indicated in red, and extent of 2015 event indicated in green (Landrø, Mikkelsen & Jaedicke, 2017)

Thereafter, NVE assumes increased weight from the initial deposition caused the triggering of a secondary and ultimately hazardous avalanche (Landrø, Mikkelsen, & Jaedicke, 2017).

The preconditions leading up to the event was in this instance divers, resembling those leading up to the prior event. The period from 05.02 – 12.02 were characterized by temperatures above freezing, combined with 28 mm precipitation, mainly in the form of rain. In the next period from 13.02 – 19.02 the wet snow were exposed to cold temperatures, with a minimum at -21.1 °C. When such extreme fluctuations occur, a weak layer form at the surface, which in this scenario were later buried during the next precipitation event from 19.02 – 21.02 in the form of snow. In combination with strong winds (up to 25 m/s), which consequently results in the same challenges as the former event, with the already existing snow being redistributed, adding weight to the weak layer causing it to propagate (Landrø, Mikkelsen, & Jaedicke, 2017).

As a consequence of the 2015 event, NVE begun to locally forecast avalanche danger in areas of Longyearbyen with infrastructure at especially high risk. The regional danger level was assessed to a level four – which is large. However, the local assessment concluded that the probability for avalanches putting any infrastructure at risk were low due to the distance from the expected release area to the settlements. Furthermore, avalanches being released from the top of the mountain had never before been observed, and were not evaluated as likely in this scenario due to strong winds presumably causing ablation at the mountaintop (Landrø, Mikkelsen, & Jaedicke, 2017).

2 Method

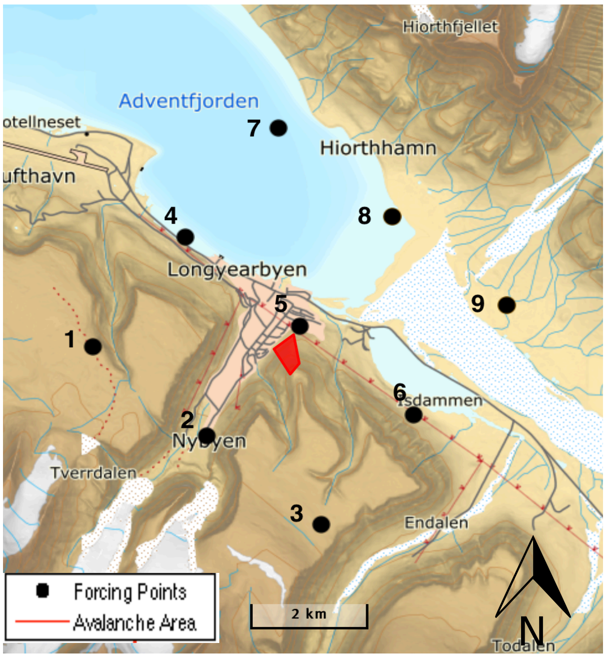

Figure 5: Approximate avalanche area, and the 9 forcing points from which forcing data are collected (Norgeskart, 2018)

Table 1: Table showing forcing points, with corresponding elevation and locations

Forcing Point	Elevation (m a.s.l.)	Latitude (°N)	Longitude (°E)
1	401.7389	78.2152	15.5036
2	311.9387	78.2008	15.5883
3	329.3321	78.1865	15.6729
4	80.3230	78.2325	15.5737
5	74.0698	78.2182	15.6586
6	103.8483	78.2038	15.7432
7	29.9458	78.2498	15.6441
8	62.0604	78.2354	15.7290
9	56.2648	78.2210	15.8136

The method will mainly be divided into two parts. In the first instance, the thesis will be predicated on the snow cover model CROCUS to simulate the snow cover at nine adjacent points to site of the two relevant events with forcing data from AROME-Arctic (Fig. 5). In accordance with Durand, Giraud, Brun, Mérindol & Martin (1999), these points are scattered throughout the general research area, representing different elevations (Table 1), securing the premises in which an attempt to detect the best approximation to the prevailing conditions are possible. Unfortunately, aspect will not be considered in this thesis, because it was discovered within the forcing that all values equaled zero degrees from north. Consequently leading to a situation whereas this variable had to be disregarded. However, from the analysis of the results from the simulations it will be possible to evaluate whether the model successfully was able to recreate the unstable conditions that are now known to be true. If the model fails to recreate these conditions the first part of the method will be expanded to potentially make the model perceive the avalanche danger. Therefore, if the hypothesis presented in section 1.1 turns out to be correct; concerning the accumulation from blowing snow to be underrepresented in the model.

This will be accounted for by increasing the accumulation from snowfall in the model gradually to force the simulation closer to the observed situation. This process will potentially be executed in the relevant month only and in addition serve as a sensitivity analysis, which will be revisited in the discussion. From this context, the method can be divided into a qualitative and a quantitative part. The quantitative part, concerning the quantification of the snow cover and the output of the model, and the qualitative part, concerning the analysis of the quantified results.

The qualitative process will specifically involve assessing the model systems performance in relation to observations and the simulated avalanche danger and furthermore consider whether these results have the potential to assist future avalanche forecasters stability assessments. In that regard, an introduction to model workflow and how it threats which variables to visualize the simulated snow cover, in addition to a description of relevant avalanche theory are necessary to appropriately conduct these evaluations. Furthermore, because insecurities are associated with forcing input (Vikhamar-Schuler, Müller, & Engen-Skaugen, 2011) the qualitative part will assess whether AROME-Arctic is suitable for the model system with this specific purpose.

2.1 Program Workflow

Crocus was originally launched in 1989, and have since then, been under constant development. The initial model aimed to simulate energy and mass evolution of snow cover at a given location as a function of the following meteorological conditions: Precipitation, air temperature, humidity, wind velocity and incoming short wave and long wave radiation (Brun, Martin, Simon, Gendre, & Coleou, 1989). The model proved itself efficient in simulating snow temperature, liquid-water content and density profiles. However, the model was limited because its inability to simulate snow cover stratigraphy over time (Brun, David, Sudul, & Brunot, 1992). Snow metamorphism, both dry and wet depends on temperature, density and liquid-water profiles in each individual layer (Colbeck, 1980). Since the initial model from 1989 proved itself efficient simulating these variables over time it could surely be able to simulate metamorphism as a function of these. This project finally lead to a way of quantifying wet and dry snow metamorphism and successfully implementing it in the model in 1992 (Brun, David, Sudul, & Brunot, 1992). Nevertheless, since these original publications the program has seen many upgrades including the implementation in SURFEX. SURFEX computes the exchange of energy and mass between different types of surface and the atmosphere. It includes in particular the land surface scheme ISBA, which allows straightforward thermodynamic coupling of the snowpack scheme to the soil component of the land surface model. Allowing for quantifications of thermodynamic interactions between the snowpack and ground component (Vionnet, et al., 2012).

The model system utilized in this study is the snowpack scheme CROCUS within SURFEX. This model needs the following variables to run: (i) air temperature, specific humidity and wind speed at known height above ground; (ii) incoming radiation: direct and diffuse short wave and long wave; (iii) precipitation rate, split between air and snow; and (iv) atmospheric pressure. These inputs may be derived directly from local observations, atmospheric models or reanalyzes. As a result from these driving variables the output will describe each layer by its thickness D, heat content H, density ρ, and age A (Vionnet, et al., 2012). To describe snow evolution as a function of continuous parameters additional variables are used to describe the evolution of snow grains using metamorphism laws. Dendricity d, sphericity s and grain size $g_{S.}$ Whereas dendricity describes the original crystal shapes remaining in a snow layer and sphericity describes the ratio of rounded versus angular shapes. An additional historical variable (h) indicates whether it once was liquid water or faceted crystals in the layers. The variables d, s, g_s and h are termed the grain variables, and are used to diagnose the snow type (Brun, David, Sudul, & Brunot, 1992). Most of these new conventions will be revisited and described in separate sections bellow.

In this thesis the driving variables, also known as forcing data will be acquired from met.no's weather forecast model AROME-Arctic. AROME-Arctic is a regional short-range high-resolution forecasting system for the European Arctic with 2.5 km grid spacing and sixty-five vertical levels (Met.no, 2017). Meaning that the input data are acquired from previous forecasts, and not already registered in situ observations from automatic weather stations. The decision is based on the fact that forecasts provide superior density in addition to avoiding holes in the dataset in comparison with automatic weather stations. Because Norway has a less dense station networks, there is a greater need for models in general (Vikhamar-Schuler, Müller, & Engen-Skaugen, 2011). Furthermore, such an approach to the problem is recognized as more realistic in an avalanche-forecasting scenario. Whereas the uncertainties regarding the forecasts are accounted for in the thesis.

The remainder of this section will aim to, on a more specific note, give a short introduction on how the program works, what variables the program aims to simulate and in what manner it does so. The program consists of forty-nine variables, which can be visualized and simulated, there would be inexpedient to give an overview of all of these variables. For that reasons there are a few selected, that would be important for this specific thesis that will be described.

2.1.1 Snowfall

When snow is falling, fresh snow layers are added to the snowpack. The model accounts for the impact of near surface meteorological conditions on the properties of falling snow. The density of freshly fallen snow is expressed as a function of wind speed U, and air temperature T_a:

$$\rho_{new} = a_\rho + b_\rho\left(T_a - T_{fus}\right) + c_\rho U^{1/2} \tag{1}$$

Where T_{fus} is the temperature of the melting point of water and a_ρ, b_ρ and c_ρ are constants. The value of ρ_{new} is further utilized to compute snowpack thickness from precipitation amount (Vionnet, et al., 2012). The parameters of equation (1) originate from a study by Pahaut (1976) at Col de Porte, in the French Alps.

2.1.2 Dynamic Evolution of Snow Layers

The dynamical evolution of the number and thickness of the numerical snow layers is a key original feature of the CROCUS snow scheme. Which aims to simulate the vertical layering of natural snowpacks in the best possible way (Brun, David, Sudul, & Brunot, 1992). A minimum number of three layers are required for solving the heat conduction through the snowpack, but there are no limitations on the maximum number of layers (Vionnet, et al., 2012). This feature is user-defined and in the case of this thesis a maximum number of fifty layers have been defined. An important point to mention is that the snowpack scheme dynamically manages different vertical grid mesh, in terms of the number and thickness of snow layers. Meaning that the number of layers and their sizes changes dynamically over time and are treated differently for different scenarios: (i) For snowfall over bare soil the snowpack is built up from identical layers, in terms of thickness and state variables. Their number depends on amount of fresh snow and the maximum numbers of layers. (ii) For snowfall over an existing snowpack, it is first attempted to incorporate the freshly fallen snow into the existing top layer, provided its grain characteristics are similar and its thickness smaller than a fixed limit. The similarity between two adjacent layers is determined from the value of the sum of their differences in terms of d, s and g_s, each weighted appropriately. If the merging is not possible, a new numerical layer is added to the preexisting one. If the number of layers reaches its maximum a search is carried out to identify two adjacent layers with satisfactory similarity coefficient. For this to be possible the model might have to minimize the criterion that governs layering definition. This merging-process will also be carried out in the scenario of no snowfall (IBID).

2.1.3 Snow Metamorphism

Snow metamorphism drives snow-cover evolution and affects all of its properties, especially mechanical properties and albedo. Before the implementation of the snow-cover model CROCUS snow metamorphism had traditionally been described from a qualitative point of view (Brun, David, Sudul, & Brunot, 1992). It is intuitively obvious why a qualitative description of snow metamorphism are useless in a numerical model, which is why there was a immediate need to describe snow metamorphism in a quantitative manner. To solve this problem Brun, David, Sudul and Brunot (1992) conducted a series of metamorphism experiments to define snow metamorphism quantitatively.

To properly implement snow metamorphism in the CROCUS snow-scheme Brun, David, Sudul and Brunot (1992) defined dendricity and sphericity, where dendricity varies from 1 to 0 and describes the part of the original crystal shapes that are still remaining in a snow layer. Sphericity also varies between 0 and 1 and describes the ratio of rounded versus angular grains. These properties, and their evolution in the snowpack will furthermore depend on the moisture content of the snowpack. Which is why quantitative metamorphism properties were defined to be dependent on whether the fresh snow are wet or dry:

Dry Fresh Snow Metamorphism:

Brun, David, Sudul and Brunot (1992) conducted forty-four experiments using six different fresh snow samples to quantify dry snow metamorphism. Their most important results relevant for this thesis can by summarized as follows:

The type of metamorphism depends on temperature and temperature gradient. If the temperature gradient is less than 5 °C m^{-1} fresh snow will evolve towards rounded crystals. If the temperature gradient is higher than 5 °C m^{-1} fresh snow evolve towards faceted crystals. Furthermore, until the whole sample is composed of either rounded or faceted crystals, fresh snow evolves alternatively towards one or the other shape when the gradient alternates through the threshold of 5 °C m^{-1}.

The quantitative results of the forty-four experiments can by described by the following equations:

When $|\nabla T| < 5°C\ m^{-1}$:

$$\frac{\delta\ dendricity}{\delta t} = -2 \times 10^8\ e^{\left(\frac{-6\ \times 10^3}{T}\right)} \tag{2}$$

$$\frac{\delta\ sphericity}{\delta t} = 1 \times 10^9\ e^{\left(\frac{-6\ \times 10^3}{T}\right)}$$

When $|\nabla T| \geq 5°C\ m^{-1}$:

$$\frac{\delta\ dendricity}{\delta t} = -2 \times 10^8\ e^{\left(\frac{-6\ \times 10^3}{T}\right)}(\nabla T^{0.4}) \tag{3}$$

$$\frac{\delta\ sphericity}{\delta t} = -2 \times 10^8\ e^{\left(\frac{-6\ \times 10^3}{T}\right)}(\nabla T^{0.4})$$

Wet Fresh Snow Metamorphism:

Wet snow metamorphism can satisfactory be described by the following equations, where t is time and θ is expressed in percent water per mass (Brun, David, Sudul, & Brunot, 1992).

$$\frac{\delta\ dendricity}{\delta t} = \frac{-1}{16}\theta^3 \tag{4}$$

$$\frac{\delta\ sphericity}{\delta t} = \frac{1}{16}\theta^3$$

2.1.4 Compaction

The snow layers settle upon the combined effect of snow metamorphism, and the weight of the overlying layers, applying force to a specific layer. The settling is expressed in the following equation:

$$\frac{dD}{D} = \frac{-\sigma}{\eta} dt \qquad (5)$$

Where D is the layer thickness, σ the vertical stress (computed as the weight of overlying layers), dt the model time and η the snow viscosity. Furthermore, the vertical stress from the weight of overlying layers for each layer is expressed as follows:

$$\sigma_i = \sum_1^{i-1} g \cos(\Theta)\rho(\mathrm{i})\mathrm{D}(\mathrm{i}) \qquad (6)$$

Where Θ is the local slope and g is terrestrial gravitation, $\rho(\mathrm{i})$ and D(i) are density and thickness of the relevant layer.

Furthermore, the viscosity η is described as a function of snow density, temperature, liquid water content and grain type and is given as follows:

$$\eta = f_1 f_2 \eta_0 \frac{\rho}{c_\eta} e^{(a_\eta(T_{fus} - T) + b_\eta \rho)} \qquad (7)$$

Where η_0, a_η, c_η and b_η are constants. f_1 and f_2 are correction factors that adjust the snow viscosity based on snow microstructure properties. They account for the decrease of viscosity in presence of liquid water and the increase of viscosity with angular grains (Vionnet, et al., 2012).

2.1.5 Wind Drift

Under strong wind conditions, snowflakes break upon collision between each other and with the snow surface (Sato, Kosugi, Mochizuki, & Nemoto, 2008), so their properties differentiate from purely fresh snow. This challenge is accounted for in the model in a simplified way, as described by Brun, Martin and Spiridonov (1997). For each type of snow, a mobility index and wind threshold above which snowdrift occurs are calculated. If, at a grid point, wind speed exceeds the threshold corresponding to the snow cover that is simulated at this grid point, it is assumed that snowdrift occurs. Which further induce an increase in snow density and a change of its crystals. Its efficiency is expressed as a function of the wind, and its effects on snow compaction and metamorphism, which decreases exponentially as a function of depth and the mobility of the upper layer. Note that, in stand-alone mode, CROCUS does not handle explicitly wind-induced snow redistribution since grid points are threated individually from each other. (Vionnet, et al., 2012). Which is why the method potentially is in need of expansion, if the primary results are unsatisfactory. Where reaccummulated snow from wind drift can be accounted for by increased snowfall.

2.1.6 Snow Albedo and Transmission of Solar Radiation

Solar radiation is handled in three separate spectral bands: ([0.3-0.8], [0.8-0.15], [1.5-2.8] μm). Firstly, the albedo is computed in each band, as a function of the snow properties in the top 3 cm of the snowpack. The spectral albedo depends only on the optical diameter, d_{opt}, of snow. This is empirically derived from d, s and g_s, based on experimental work by Sergent et al. (unpublished):

$$d_{opt} = \begin{cases} 10^{-4}[d + (1-d)(4-s)] & Dendritic\ case \\ g_s \times s + (1-s) \times \max\left(4.10^{-4}, \frac{g_s}{2}\right) & Non-dendritic\ case \end{cases} \quad (8)$$

Once the spectral albedo is calculated in every spectral band the incoming radiation is depleted by its value, and the remaining part penetrates into the snowpack and is gradually absorbed assuming an exponential decay of radiation with increasing snow depth. The solar flux Q_s, at a depth z below the snow surface is expressed as follows:

$$Q_s = \sum_{k=1}^{3}(1-\alpha_k)R_{sk}e^{-\beta_k z} \quad (9)$$

Where R_{sk} represents the incoming solar radiation, α_k the albedo, and $\beta_k$the absorption coefficient in the spectral band k (Vionnet, et al., 2012).

2.1.7 Surface Fluxes and Surface Energy Balance

The surface fluxes govern the surface energy balance. The surface fluxes are divided into the latent heat flux, LE, and the sensible heat flux, H_F. Firstly the latent heat flux are written as:

$$LE = (\chi L_f + L_v)\rho_a C_H U[q_{sat}(T_s) - q_a] \quad (10)$$

Where L_f and L_v represents the latent heat of fusion and vaporization, respectively. q_a is atmospheric specific humidity, $q_{sat}(T_s)$ is the saturation specific humidity above a flat ice surface at the temperature T, and T_s is snow surface temperature. χ denotes the ratio between the solid and liquid phases of the turbulent mass exchanges between the snow surface and the atmosphere.

Furthermore the sensible heat flux are described in the following equation:

$$H_f = \rho_a C_p C_H U \left(\frac{T_s}{\Pi_s} - \frac{T_a}{\Pi_a}\right) \tag{11}$$

Where C_p is the specific heat of air, and Π_s and Π_a are Exner functions for the surface and the atmosphere. Lastly C_H represents the turbulent exchange coefficient (Vionnet, et al., 2012).

2.1.8 Resolution of Snow Temperature Profile

To compute the snow temperature profile, the heat diffusion within the snow cover is computed by using the backward-difference integration scheme of ISBA-ES (Boone & Etchevers, 2001). The snow effective thermal conductivity, k, is expressed in the following equation, following the works of Yen (1981).

$$k = k_{ice} \left(\frac{\rho}{\rho_w}\right)^{1.88} \tag{12}$$

The net heat flux, at the snow-atmosphere interaction combines the turbulent fluxes, with the net radiative components. Referring to short and long wave radiation. Furthermore the model also includes a precipitation heat advection term for when it is raining.

At the bottom of the snowpack, CROCUS is fully coupled to the soil component of the land surface model ISBA via a semi-implicit soil-snow coupling which conserves heat and mass. The conduction heat-flux at the snow/soil interface is explicitly modeled and depends on the temperature gradient between the snow bottom and the upper soil layer (Vionnet, et al., 2012).

2.1.9 Snow Melt

CROCUS handles melting in 3 different manners, depending on the amount of melt that occurs between two time steps. (1) Complete melt of entire snowpack, (2) complete melt of one or multiple layers, and (3) partial melt of individual layers.

1. The first routine calculates the new heat content of the snowpack from the new temperature and density profile. Looking at the difference between two time steps. Further it compares this energy to the amount of energy needed to melt the entire snowpack, from which possible sublimation have been subtracted. If the available energy exceeds this energy the entire snowpack melts and the routine further computes the corresponding impact on the ground heat and water fluxes, to ensure the conservation of energy and mass, while taking into account the vapor exchange between the vanishing snowpack.

2. The second routine accounts for the case when one or several snow layers completely melt between two time steps, before the computation of the partial melting/refreezing inside each snow layer. First the routine compares the heat content of each snow layer to the amount of energy that is necessary for the complete melt of its ice mass. If this energy exceeds this value the snow layer is merged with the underlying layer, except for the bottom layer, which might merge with the overlying layer.

3. The last routine is run after the two previously explained routines, which means that the available energy from the new temperature of any snow layer is not large enough to melt it completely. When the new temperature of a layer exceeds the melting point, the temperature is turned to the melting point and the corresponding energy is consumed for ice melting. The corresponding melt water is added to the liquid water content of the layer. The dry density of melting layers is conserved at this stage and their thickness decreases accordingly (Vionnet, et al., 2012).

2.1.10 Water Flow and Refreezing

Water in a snowpack, and the potential freezing of water is important to the energy balance of a snowpack. Water might freeze and liberate latent heat to increase the temperature of the snowpack, which can further promote melting (Cuffey & Paterson, 2010). To handle the issue of water flow and refreezing in an expedient manner the model first updates the liquid water content of the surface snow layer by including contributors from rainfall and liquid condensation or evaporation at the surface. Then, it calculates the amount of energy available for liquid water refreezing from the new temperature of each snow layer. If freezing do occur in a layer, its liquid water content is decreased and temperature adjusted accordingly. The water flow through the snow layer is then simulated, which is modeled as a series of reservoirs, with one for each layer (Vionnet, et al., 2012). Water flow occur when the liquid water content exceeds the maximum liquid water holding capacity, which is expressed as 5% of the total pore volume (Pahaut, 1976). The model considers gravitational flow only, and neglects the formation of capillary barriers (Jordan, 1995). The water flow solution procedure starts from the upper-most layer and proceeds downward. Water entering a layer refreezes if thermodynamics allows it. If a layer can no longer freeze present water, unfrozen water is retained up to the maximum holing capacity. Water flow processes do not impact the layer thickness (Vionnet, et al., 2012).

2.1.11 Snow Sublimation and Hoar Deposition

To account for sublimation and hoar deposition the model adds or subtracts to the snow surface layer the ice amount corresponding to the turbulent vapor fluxes. The surface snow layer is adjusted accordingly while the density is assumed to stay unchanged. Which assumes that at this stage CROCUS does not represent the specific properties of surface hoar.

2.2 Snowpack Stability Evaluations

In the interest of assessing CROCUS' performance, both in regard to accuracy, and ability to indicate avalanche danger correctly, a natural approach is to compare the model output to field observations. One day prior to the 2017 event, NVE recorded a snowpit and conducted a extended column test in the same slope the destructive event later took place (Landrø, Mikkelsen & Jaedicke, 2017). These observations can be utilized as correctional tools to evaluate both aspect of the first research question from section 1.2. However, such abundance of quantitative observations could not be obtained regarding the 2015 event. Therefore, another approach is imminent. Because internal snowpack conditions and snowpack stability is dependent variables (Temper, 2008: Buser, Föhn, Good, Gubler, & Salm, 1985), and one aspect regarding the scope of this study concerns the models utility as an avalanche danger forecasting tool, it is neccessary to interpret the stability of the simulated snowpack. This process will be conducted regardless of the existense of correctianal tools and ultimately make it possible to comment both aspects of the first research question, regarding ability to reproduce snowpack stratigraphy and indicate avalanche danger at the correct time step.

Therefore, an introduction on how to conduct snowpack stability evaluations, from snowpack stratigraphy is necessary. Stability evaluation means to assess the probability of avalanche release for the snow conditions under consideration (Schweizer & Wiesinger, 2001). It should very much be mentioned that there are no rigorous way to interpret a snow profile, and it is largely experienced based (Bair, Simenhois, van Herwijnen, & Birkeland, 2015). Therefore, the method will not necessarily be absolute, but rather guidelines on how to interpret the output of CROCUS. Furthermore, there are several factors that often are deemed important in traditional avalanche danger assessment, such as occurrence of past avalanches (McClung & Schaerer, 1993). This specific aspect will not be considered in this thesis because it is not defined within the primary scope. Nevertheless, the following paragraphs will revolve around what output data from the model that will be weighted as most important concerning avalanche danger assessment, and in what way they are assumed to influence snowpack stability.

2.2.1 Depth

Snow depth observations have several purposes. To determine whether or not there is enough snow to cover terrain and vegetation anchors so that avalanches can start easily, to monitor snowpack settlement, and to observe snow distribution across terrain. A basic requirement for avalanches is enough snow in the avalanche starting zone and tracks to reduce surface roughness features. Furthermore, avalanches can only be classified as a hazard when it threatens anything of value to humans. Because an analysis of snow depth indirectly says something about the potential volume of an avalanche, it can further say something about whether the potential avalanche might be large enough to reach a settlement (McClung & Schaerer, 1993).

2.2.2 Temperature

McClung and Schaerer (1993) claims that snow temperature affects stability in two ways: Firstly, snow stiffness increases rapidly with decreasing temperature and at the same time brittleness increases, causing increased potential for rapid fracture propagation. This agrees with the claims of Ferguson (1984), which suggest that unstable snow is colder than stable snow. Yet, one should keep in mind that in dry conditions the snow temperature alone does not reveal potential instability (Schweizer & Wiesinger, 2001). This is because in low temperatures (<-5 °C) bond formation is slow, causing existing weaknesses to potentially persist for a long time (McClung & Schaerer, 1993). Even though low temperatures don't cause instabilities (Schweizer & Wiesinger, 2001), they can most certainly sustain them. Compared to the cold conditions one should keep in mind that strength decreases significantly when the temperature approaches 0°C (McClung & Schaerer, 1993).

Secondly, temperature and its gradient control the metamorphism of the snow, which in turn, influences its strength. For example will a weak gradient increase the strength at a rate that increases with the temperature and depends on the shape and size of snow grains. The rounding, sintering and settling is slow at low temperature and for large crystals, faceted grains, surface hoar and depth hoar. On the other hand will a strong temperature gradient cause the snow to loose strength with facet formation (McClung & Schaerer, 1993).

Several specific threshold gradients have been proposed in different papers, attempting to quantify metamorphism. Colbeck (1993) claimed that the threshold of which metamorphism favors towards rounded or faceted grains were 0.1 – 0.2 °C cm^{-1}. On the other hand did McClung & Schaerer (1993) claim that the same threshold was 10 °C m^{-1}, in addition to Brun, David, Sudul and Brunot (1992) postulating the threshold to be 5 °C m^{-1}. In an attempt not to engage in cognitive dissonance, this thesis will utilize the latter threshold. Because this is the threshold of which the model utilizes, possibly resulting in increased coherence between the qualitative and quantitative part of the thesis.

2.2.3 Hardness

According to McClung and Schaerer (1993) will shear strength increases with hardness as a general rule. The issue to overcome concerning hardness is that the most frequently used hardness index is the hand hardness index applied in field. This kind of measuring is vastly subjective, but can still give some kind of indication. Where weak layers usually are characterized as soft and ranging from fist to four fingers hardness. Also decreasing hardness with increasing depth is an indicator of instability. In addition, critical weak layers are frequently sandwiched between harder layers (Schweizer & Wiesinger, 2001). The uncertainties regarding the traditional method of obtaining hardness approximations have to be considered, because the study in some instances will compare the simulations to field observations. However, of upmost importance is the relative hardness within the snowpack.

2.2.4 Ram Profile

The ram profile shows the vertical distribution of penetration resistance or ram hardness of the snowpack. The hardness profile is characterized as one out of ten types of profiles (Schweizer & Wiesinger, 2001) (Fig. 6). DeQuervain and Meister (1987) have given a first classification. The profile types 1 – 5 all have a weak base, whereas the profile types 6 – 10 are well consolidated at the

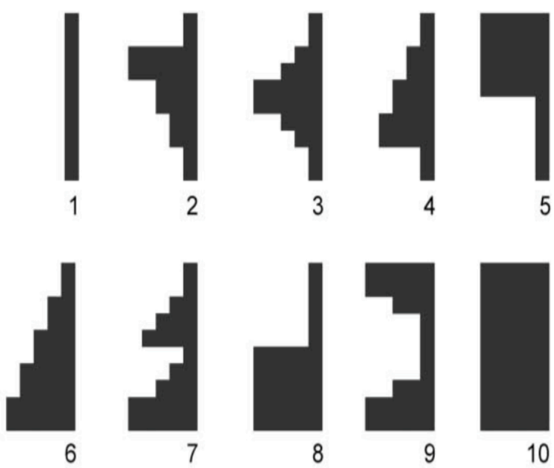

Figure 6: The 10 different hardness profiles (Schweizer & Wiesinger, 2001)

bottom. The profiles types 1, 5, 7 and 9 indicate potential instability. Profile types 6 and 10 represent in general stable conditions, whereas types 2, 3, 4 and 8 cannot be assigned definitely, but all show some potential, but depending on the condition, usually less critical weakness. The presence of a weak base of depth hoar is not conclusive on its own. If the profile is well consolidated in its middle part (belly-shaped profile in combination with a weak base), this points to good or very good stability (Schweizer & Wiesinger, 2001).

2.2.5 Grain Size and Type

Snow tends to have high strength when grains are small and round. Snow with larger grains tends to have a lower strength than grains with the same shape, but smaller size (McClung & Schaerer, 1993). This is because the larger the grains, the lower the number of bonds per unit volume, particularly in combination with persistent grain types. Furthermore, one should keep in mind that significant differences in grain size from one layer to another usually are unfavorable (Schweizer & Wiesinger, 2001). Grains with angled surfaces and an elongated shape, such as, surface hoar, faceted grains, depth hoar, needles, plates and columns often indicates weak snow. Graupel usually consists of large spherical grains, which often form weak snow (McClung & Schaerer, 1993).

2.2.6 Liquid Water Content

Wet snow tends to be weak, and strength decreases with the amount of free water in the snow (McClung & Schaerer, 1993). However, until the snowpack is not (or not at least partly) isothermal, the amount of liquid water is hardly considered relevant for instability assessment in generally dry snow conditions (Schweizer & Wiesinger, 2001).

2.2.7 Density

Strength tends to increase with density, but hardness is a more sensitive indicator when it comes to stability work. Densities are most useful to estimate the load on a weak layer and should not be used as the only indicator for weak layers (McClung & Schaerer, 1993). In general, dense (warm) snow on top of loose (cold) snow is unfavorable, but this is usually recognized by the hardness or grain size (Schweizer & Wiesinger, 2001).

2.2.8 Layer Thickness

A snowpack with many thin layers is in general rather unstable than a snowpack that only consists of a few relatively thick layers. Weak layers are often very thin (millimeters), but are usually less than a few centimeters. The closer the weak layer is to the surface the more critical it has to be considered in view of skier triggering. Slab thickness can also vary from centimeters to meters. The thicker and harder the slab overlying the weak layer, the more unlikely is skier triggering (other factors being equal). On the other hand a thick slab on a weak layer may produce a spontaneous avalanche as the slab increases due to loading (Schweizer & Wiesinger, 2001).

2.2.9 Extended Column Test

Because NVE conducted an extended column test prior to one of the relevant events (Landrø, Mikkelsen, & Jaedicke, 2017), and this data will be applied in the thesis, it is pivotal to give a short introduction to this kind of destructive stability testing. The primary principle of such testing is to attempt to simulate a small failure that can be correlated to slope scale avalanche danger. Specifically, an extended column test involves a 30 cm upslope and a 90 cm cross slope beam that is isolated from the surrounding snowpack and then loaded by placing a shovel on top of the beam, and tapping from the wrist, elbow and shoulder. The final amount of taps, and the depth of the potential propagation provide crucial information on the general stability and location of potential weak layers in the snowpack (Bair, Simenhois, van Herwijnen, & Birkeland, 2015).

3 Results

In this section of the thesis, the quantified results from the simulation will be presented. In most cases, regarding surface plots particularly, there would be tremendously inexpedient to present all visualized variables at all locations, due to the sheer quantity of figures. Instead, in accordance with Durand, Giraud, Brun, Mérindol and Martin (1999) one representative figure will be presented, when there is good agreement between all nine locations. If that's not the case, there will be presented more than one figure. Meaning that all surface plots being presented demonstrate prevailing main characteristics regarding stratigraphy recognized at multiple locations.

3.1 2015 Event, First Simulation

In this subsection the results form the 2015 event will be presented, organized after visualized variable.

3.1.1 Thickness Profiles

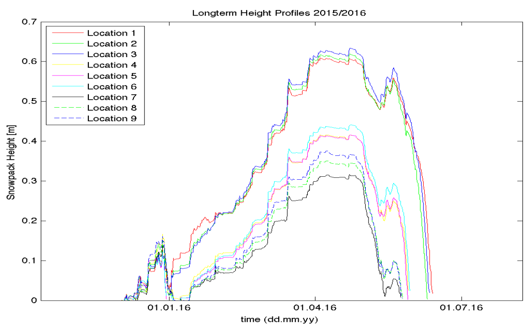

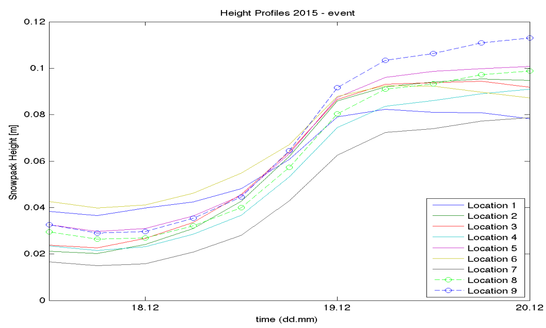

Figure 7a: Seasonal thickness profiles, 2015, all locations. Figure 7b: Thickness profiles, 2015 event, all locations

The figures show the simulated snowpack height profiles for all nine locations. Seasonal (Fig. 7a), and for the relevant step of 2015 (Fig. 7b). Looking at the seasonal plot reveals increasing differences in height between the locations with two distinct trends. However, at the time of the event all locations seem to agree well on the height of the snowpack. Even though the biggest disagreements between the simulations are more than 100 % (location 6 and 7 at 18.12), the difference is just around 2 cm. Furthermore the model seems to satisfyingly simulate the increase in snow depth the night up to the event (19.12), where all locations display a significant increase in depth. Looking at location 7 with the most extreme increase in depth from 3 cm to 11 cm, which is an overnight increase of 528 %.

3.1.2 Temperature Profile

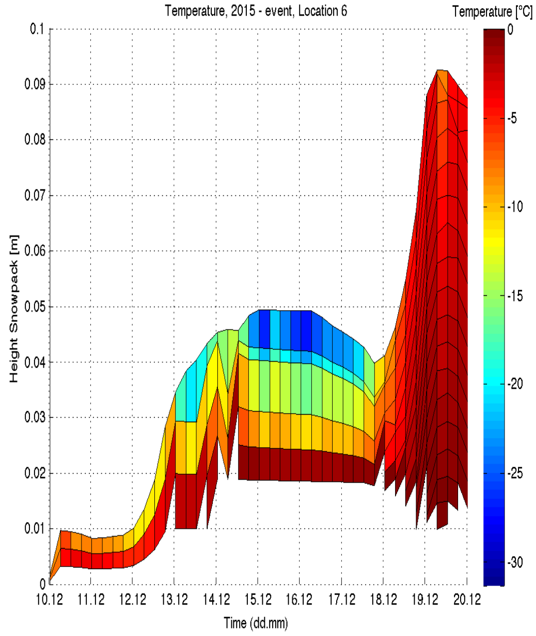

Figure 8: Temperature profile, 2015 event, location 6

Figure 8 displays temperature stratigraphy the days leading up to the event. The trend points to significantly increasing temperatures in the uppermost layers especially. Where the temperatures increase with more than 20 °C in just a couple of days. Combined with the already mentioned significant increase in thickness. Furthermore the cold snowpack in the days prior to the event reflects much more divers temperatures than the bigger, more uniformly warmer snowpack right before and during the event.

3.1.3 Temperature Gradient

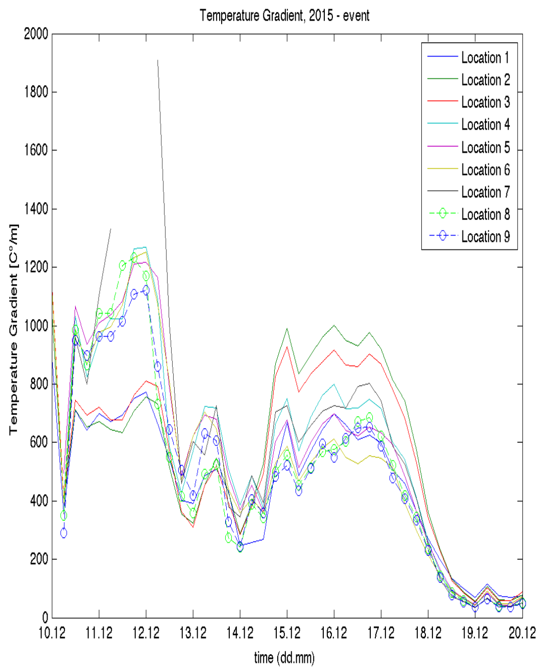

Figure 9: Temperature gradient, 2015 event, all locations

Figure 9 presents the temperature gradient for all locations the days leading up to the event, and including the event. The figure reflects a consensus between all locations, and objectively high temperature gradients, with values ranging up to 10 °Cm^{-1}. When the event itself transpires the temperature gradient have become low, relative to the previous values, reflecting a more homogeneous snowpack, temperature vise. There is also noted a discrepancy between several locations at two time steps. However, both these values are considered high and will have the same implications to the interpretation.

3.1.4 Grain Type Profile

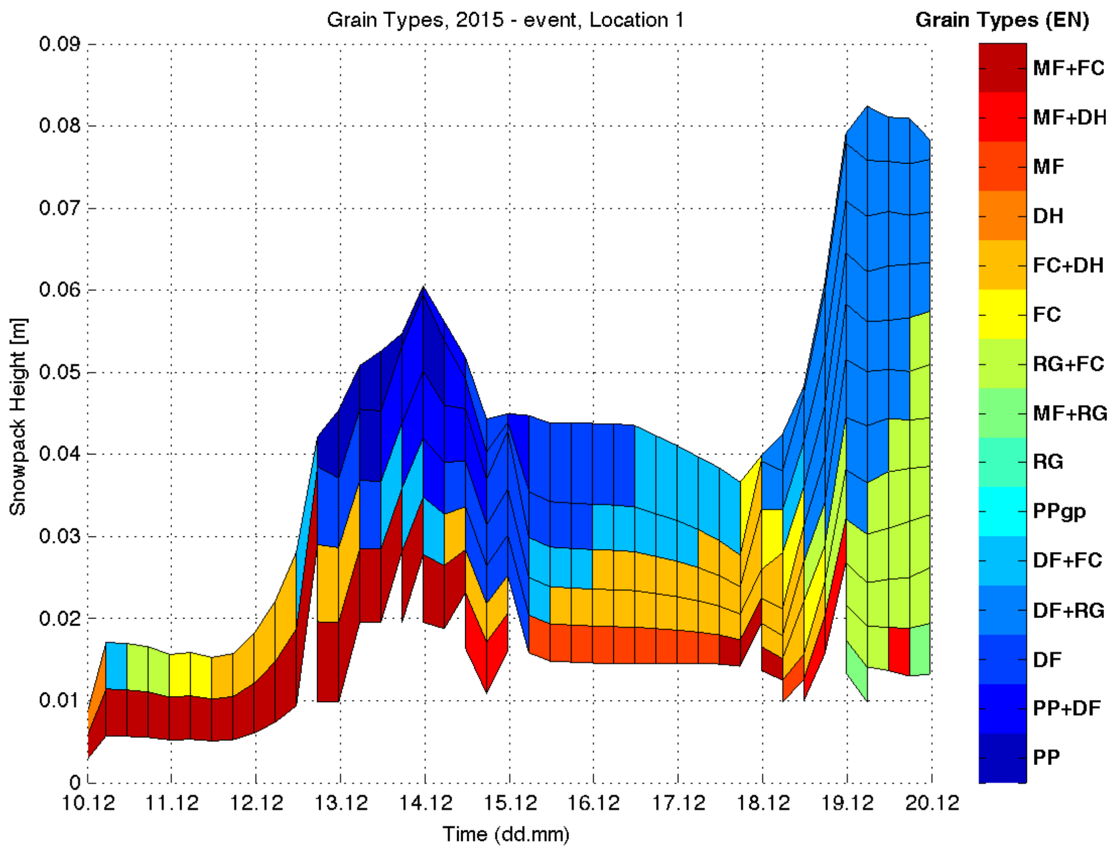

Figure 10: Grain types, 2015 event, location 1

Figure 10 demonstrates the simulated grain type stratigraphy the days leading up to, and including the event. The figure revels what kind of snow the rapid increase in snowpack thickness consists of. Which seem to be mostly decomposed and fragmented particles (DF). Furthermore, coinciding with the cold surface layers from figure 8, an evolution at the surface, from decomposed and fragmented particles into a surface layer also including facets are observed. These surface facets are combined with a layer consisting of depth hoar and facets at 17.12. During the heavy precipitation event from 18.12 – 19.12 these layers transform into a layer containing facets and rounded grains. However, it should be noted that the facets are present in all of these stages, from right after the cold period begins and until after the snowpack turns significantly warmer and deeper.

3.1.5 Grain Size Profile

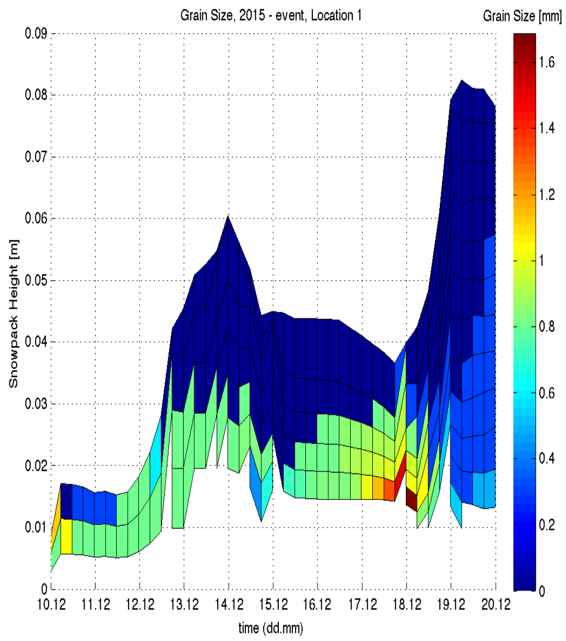

Figure 11: Grain size, 2015 event, location 1

Figure 11 shows grain size stratigraphy over time in the days leading up to, and including the 2015 event. The overall trend is vertically increasing grain sizes from the surface layers. This statement seems to hold for all locations, and the hours representing the event itself. The horizontal evolution reflects decreasing grain size in the sub surface layers as the major precipitation event prior to the avalanche event occurs.

3.1.6 Ram Hardness Profile

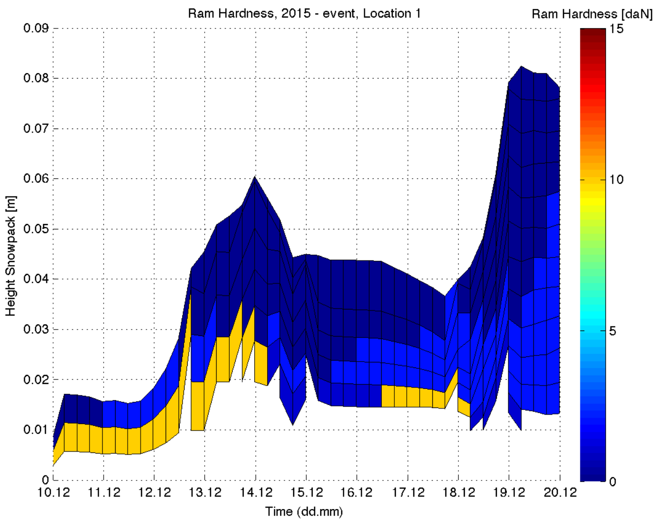

Figure 12: Ram hardness, 2015 event, location 1

Figure 12 displays the vertical hardness distribution in the snowpack over time. The overall trend at all locations reflects increasing hardness with increasing depth. However, it should be noted that the hard layer at the bottom of the snowpack prior to the event disappears and are replaced by a softer layer. This soft layer is harder than the overlying layer, but nevertheless it is objectively noted as relatively soft, compared to the overall scale of things. This soft layer is also observed to grow in size as the precipitation event prior to the avalanche event occurs.

3.1.7 Density Profile

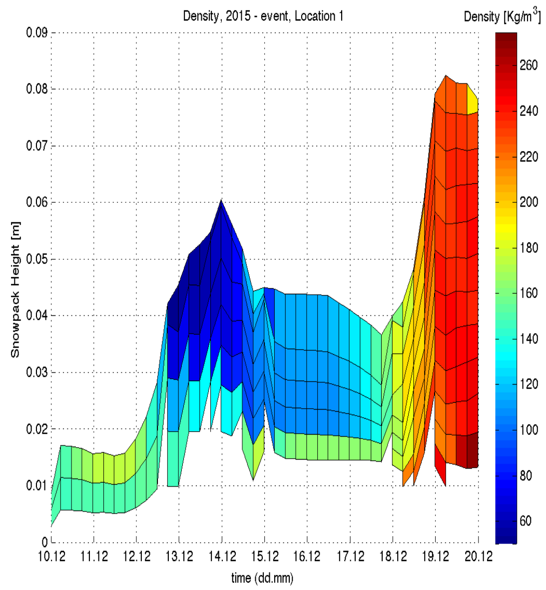

Figure 13: Density profile, 2015 event, location 1

Figure 13 demonstrates the stratigraphic development of density over time in the snowpack, for the days leading up to and including the event. As the major precipitation event prior to the event occur, the figure reflects an overall increase in density in the entire snowpack. Where the snowpack evolve from a shallow, light snowpack, into a much bigger and overall denser snowpack.

3.1.8 Liquid Water Content

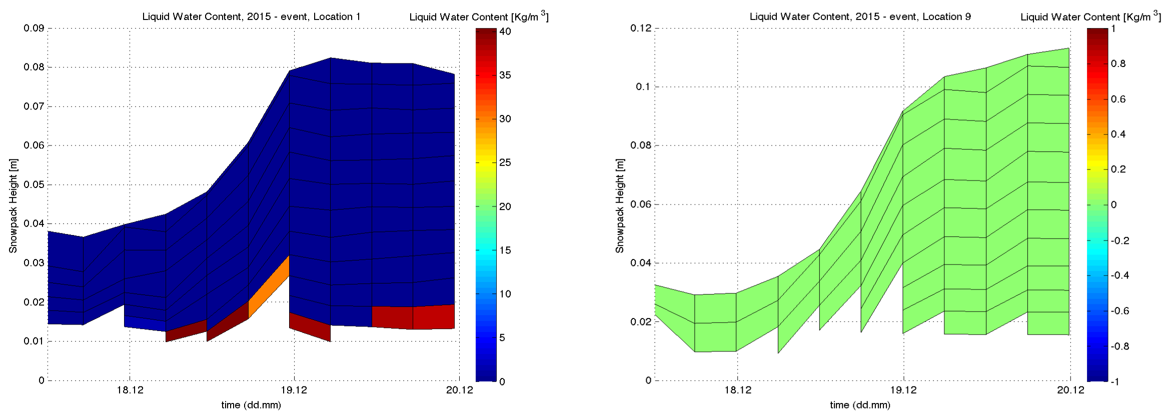

Figure 14: LIquid water content, 2015 event, location 1 and 9

Figure 14 displays liquid water content for location 1 and 9 in the snowpack over time. The general trend is virtually no liquid water stored in the snowpack. Some locations had a tremendous increase in liquid water content in the bottommost layers during and after the big precipitation event. For that reason both figures are displayed here. However, the general trend and overall impression is no liquid water in the majority of the snowpack, and furthermore the layers that might be susceptible to propagation.

3.2 2015 Event, Second Simulation

In this subsection, selected results, from the second simulation in relation to the 2015 event will be presented.

3.2.1 Sensitivity Analysis – Thickness Profiles

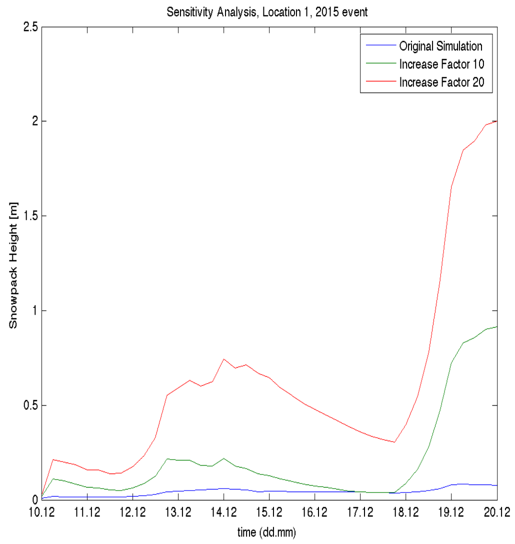

Figure 15: Thickness profiles, 2015 event, precipitation factor differentiate

Figure 15 provides a comparison of snowpack thickness between the simulations. Whereas the height profile representing the original simulation are visualized in blue. Green when precipitation is increased tenfold and lastly the red line represents when precipitation is increased with a factor of twenty. It is clear that there is a non-linear relationship between precipitation and snowpack height. Because the height of the snowpack does not increase twenty times as precipitation increase with the corresponding value.

3.2.2 Temperature Profile

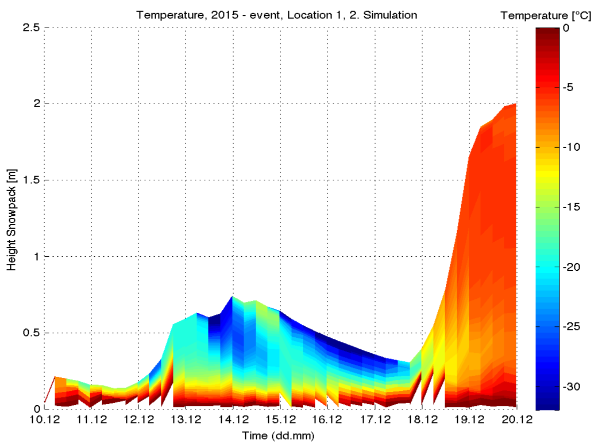

Figure 16: Temperature profile 2015 event, location 1, precipitation increased with factor 20

Figure 16 visualizes the temperature profile concerning the second simulation when precipitation is increased twentyfold. The pattern is very much similar to the pattern in the previous simulation, specifically Figure 8. The cold snowpack transitions into a much bigger, and warmer snowpack. The final snowpack representing the event is a much more homogeneous snowpack with temperatures approaching 0 °C. Although some similarities are observed in relation to the primary simulation, the height of the snowpack differentiate, whereas now the snowpack reaches 2 m at the most.

3.2.3 Grain Type Profile

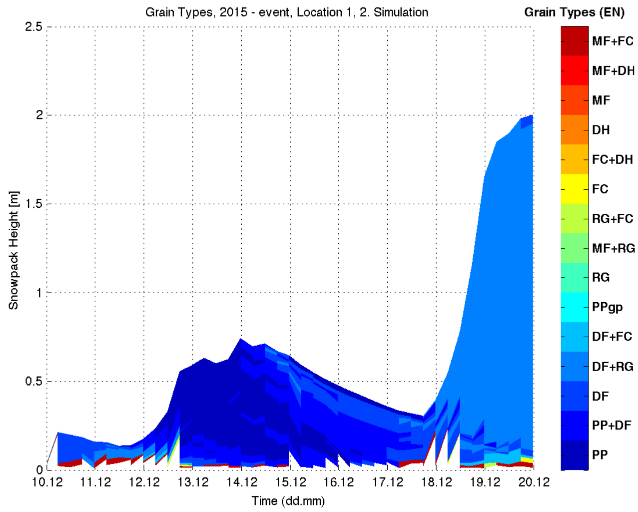

Figure 17: Grain types, 2015 event, location 1, precipitation increased with factor 20

Figure 17 visualizes the respective grain types in regard to the second simulation concerning the 2015 event, whereas precipitation is increased twentyfold. The snowpack are lacking a distinct stratigraphy. However, the tremendous increase in snowpack thickness is now projected as exclusively decomposed, fragmented and rounded grains. It is also observed that the stratigraphy from Figure 10 is preserved, but on the new scale vanishes. Two different distinct increases in thickness are also observed, at 13.12 and 19.12, consisting of PP+DF and DF+RG, respectively.

3.2.4 Density Profile

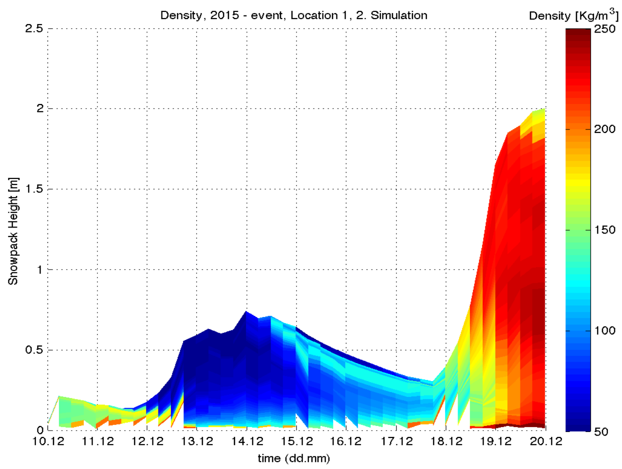

Figure 18: Density profile, 2015 event, location 1, precipitation increased with factor 20

Figure 18 visualizes density in respect to the second simulation of the 2015 event, whereas the precipitation is increased with a factor of twenty. This figure seems to very much overlap with Figure 13 visualizing density in regard to the first simulation. The same pattern is visualized in this figure as well. The lighter, shallower snowpack from 13.12–18.12 quickly transitions into a much bigger and denser snowpack. Interestingly, there is observed a slightly less dense layer at 0.5 m measured from the ground after 18.12. This layer lies underneath the much bigger and heavier layer portrayed in red. Furthermore, the snowpack are observed to be in general, much bigger compared to the initial simulation, whereas this snowpack reflects a snowpack of around 2 m.

3.3 2017 Event

In this subsection the results form the 2017 event will be presented, organized after visualized variable.

3.3.1 Thickness Profiles

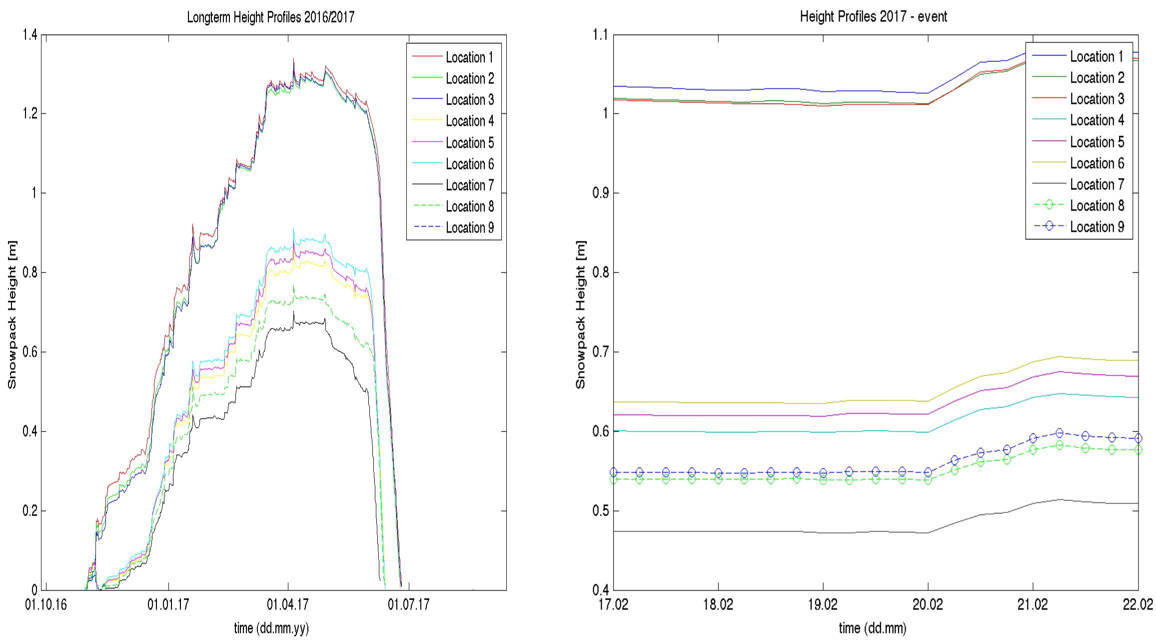

Figure 19a: Seasonal thickness profiles, 2017, all locations. Figure 19b: Thickness profiles, 2017 event, all locations.

The figures shows height profiles for all the locations in relation to the 2017 event (Fig. 19b) and a throughout the winter season (Fig. 19a). Looking at the seasonal plot reveal increasing differences in snowpack height as the season progresses. This trend is consequently represented in the specific height profile in the relevant time period. An increase in depth is observed the days leading up to the event itself. However, the different locations seem to disagree on the amount of snow. Whereas the simulation for location 1, 2 and 3 displays more than 1 m of snow, and the remaining locations display depth measurements from less than 50 cm up to about 70 cm.

3.3.2 Temperature Profiles

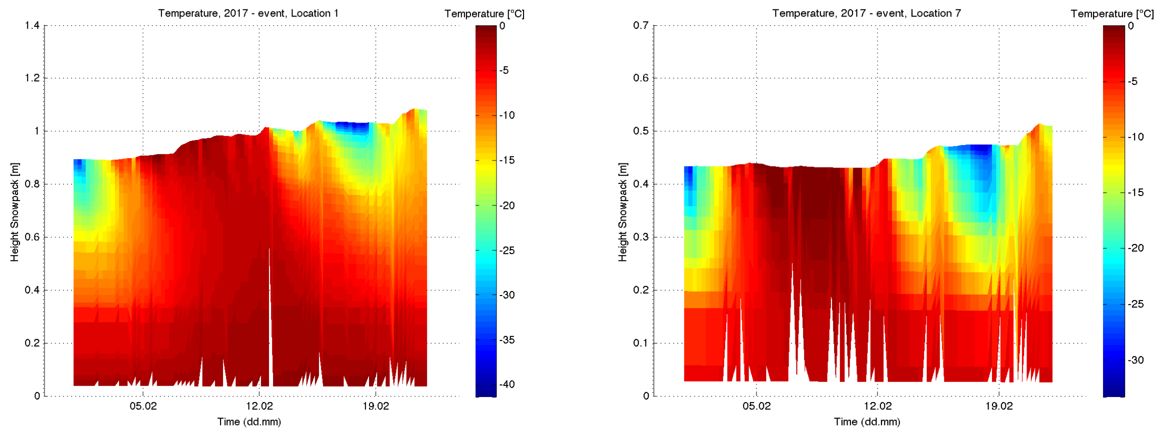

Figure 20: Temperature profiles, 2017 event, location 1 and 7

Due to the already mentioned disagreement on height, two temperature profiles are presented. However, both figures visualize the same trend. A significantly warm snowpack from 05.02–12.02 abruptly transitions into a remarkably cold snowpack. The cold temperatures penetrate roughly 20 cm into the snowpack from the surface regardless of height. Underneath these anisothermal surface layers there are observed more isothermal temperatures horizontally. Right before the event, the temperatures in the snowpack again increase significantly, simultaneously as the thickness increases.

3.3.3 Temperature Gradient

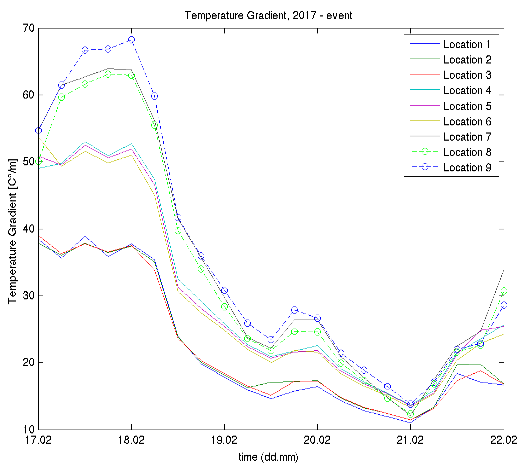

Figure 21: Temperature gradient, 2017 event, all locations

Figure 21 reflects the temperature gradient at all locations the days leading up to and including the event. There are observed some disagreements on the temperature gradients, comparing all 9 locations. Nevertheless, they all reflect a significantly bigger temperature gradient correlating with the period of overall colder temperature profiles from the previous figure. The corresponding temperature gradients, are approximately calculated to be between 40 and 70 °C m^{-1} at most.

3.3.4 Grain Type Profiles

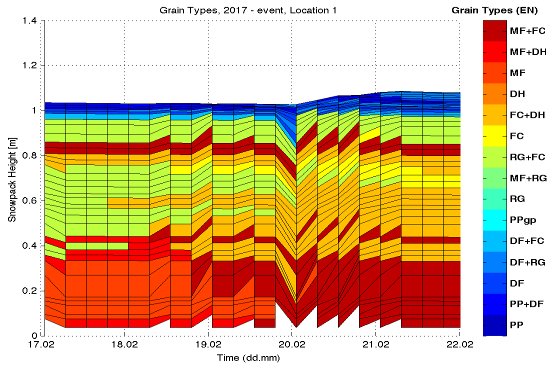

Figure 22: Grain types, 2017 event, location 1

Figure 22 displays the grain type stratigraphy the days leading up to the 2017 avalanche event, and the event itself for location 1. Prior to the event the top layer consists of decomposed and fragmented particles, together with precipitation particles (PP+DF). Followed by a layer of rounded grains and facets (RG+FC). Further, a thin layer of melt forms and facets (MF+FC) follows. This layer is again followed by a small layer consisting of facets and depth hoar (FC+DH). These thin layers are followed by a major layer in yellow, consisting of rounded grains and facets (RG+FC), which further transitions into alternating layers of melt forms paired with different grain types. It should be noted that the major, rounded grains and facet (RG+FC) layer horizontally transitions into a facet and depth hoar (FC+DH) layer just prior to the event. Where there also is observed a thin, pure, facet layer (FC). However it should be noted that during the event all layers, except the top layer contain facets.

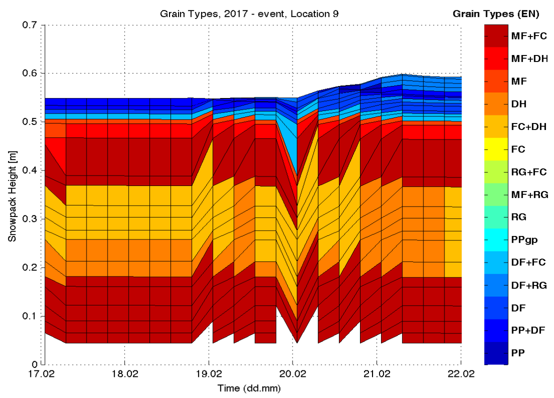

Figure 23: Grain Types, 2017 event, Location 9

Furthermore, at location 9 prior to the event there are also observed a top layer consisting of decomposed and fragmented particles in addition to precipitation particles (PP+DF). Following this layer is a thin layer with pure melt forms. This layer is again followed by alternating layers containing of facets (FC), paired with either melt forms (MF) or depth hoar (DH). This vertical pattern is however broken by a layer consisting of pure depth hoar at 20 cm from the bottom of the snowpack. The horizontal development of the snowpack is static, with no notable differences. With the exception of the facets disappearing in the combined facet and depth hoar layer (FC+DH), being replaced by a pure depth hoar (DH) layer in the hours representing the event itself.

3.3.5 Grain Size Profiles

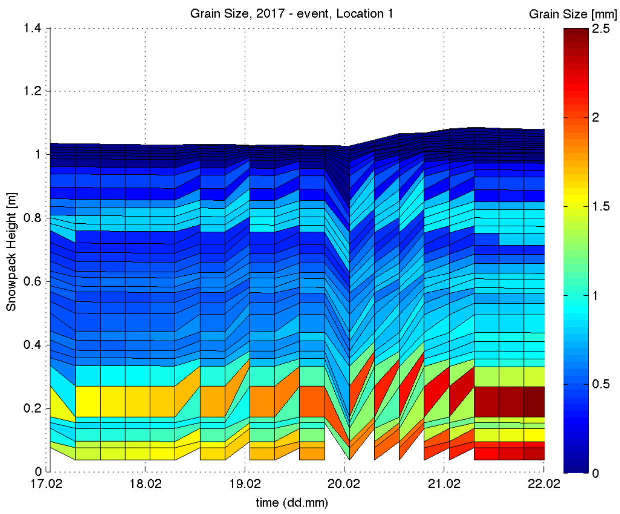

Figure 24: Grain size profile, 2017 event, location 1

Figure 24 shows grain size distribution over time at the time leading up to and including the 2017 event for location 1. The general vertical trend is increasing grain sizes from top to bottom. However, after the initial vertical increase prior to the event, there is a major small-grained layer sandwiched between two layers of greater grain size. Furthermore at the bottom of the snowpack the layers containing the biggest grain sizes are observed. Again, sandwiching layers consisting of smaller grains. The horizontal development however, reflects increasing grain sizes in all layers from 80 cm and all the way to the bottom of the snowpack. The biggest increase is observed at the layers already containing the biggest particles, at 20 cm.

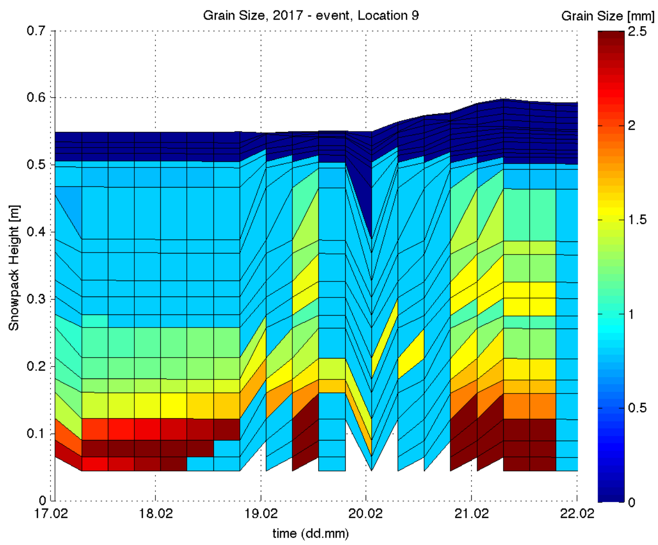

Figure 25: Grain size profile, 2017 event, location 9

Figure 25, shows the grain size distribution for the 2017 event, at location 9. Prior to the event, the figure reflects an undisputed pattern of increasing grain sizes vertically. Furthermore it displays a sudden increase horizontally at the time step representing the avalanche event. This exact same pattern is also observed a couple of days prior to the avalanche event, at midday 19.02. The most notable horizontal increase is observed at the bottom of the snowpack, were the grains in some layers increase with more than 2 mm overnight.

3.3.6 Ram Hardness Profiles

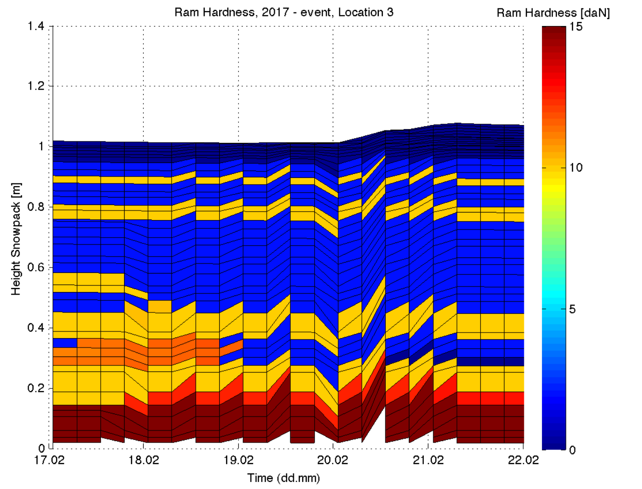

Figure 26: Ram hardness profile, 2017 event, location 3

Figure 26 displays the ram hardness stratigraphy at location 3 the days leading up to and including the event itself. Location 3 displays an alternating pattern, where the top of the snowpack, consisting of precipitation particles are the softest layer, transitioning into a slightly harder layer beneath. From here and down the ram hardness alternates the bottom of the snowpack, with a major weak layer at 40 – 80 cm from the bottom. This alternating stratigraphy ends at the bottom of the snowpack consisting of an extremely hard layer. The horizontal hardness distribution however, reflects no significant change in this variable. With one exception: At the 30 cm mark there are noted a sudden decrease in hardness in the morning hours 19.02.

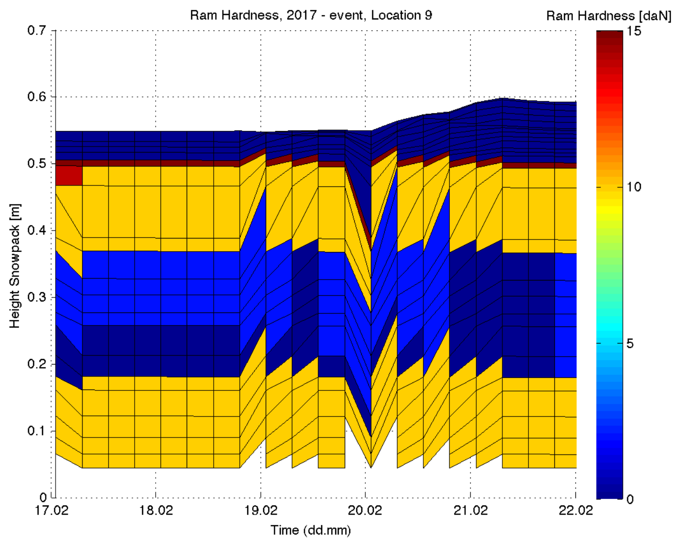

Figure 27: Ram hardness profile, 2017 event, location 9

At location 9, however, a quite different pattern is observed. Even though both location 3 and 9 reflects a soft layer at the top, at location 9 a thin, but yet tremendously hard layer follows this layer. The overall trend however is an alternating pattern, with a relatively big and soft layer observed at 20 – 40 cm sandwiched between two significantly harder layers. Furthermore, the horizontal development shows that the already softest layer becomes increasingly soft in the hours before and during the avalanche event.

3.3.7 Density Profiles

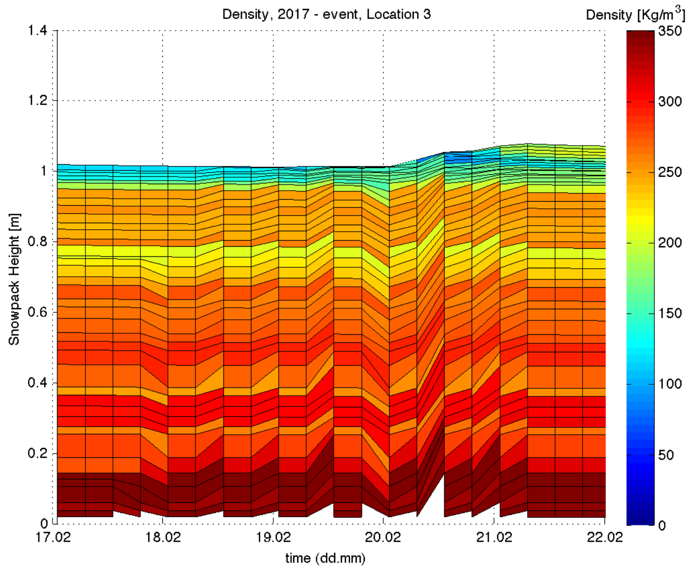

Figure 28: Density profile, 2017 event, location 3

The figure shows the density profile at location 3. There are not observed any notable horizontal development. There are, however, in general observed a pattern of increasing density with depth. With one exception of a less dense layer sandwiched between two denser ones. This layer is observed at 75 cm.

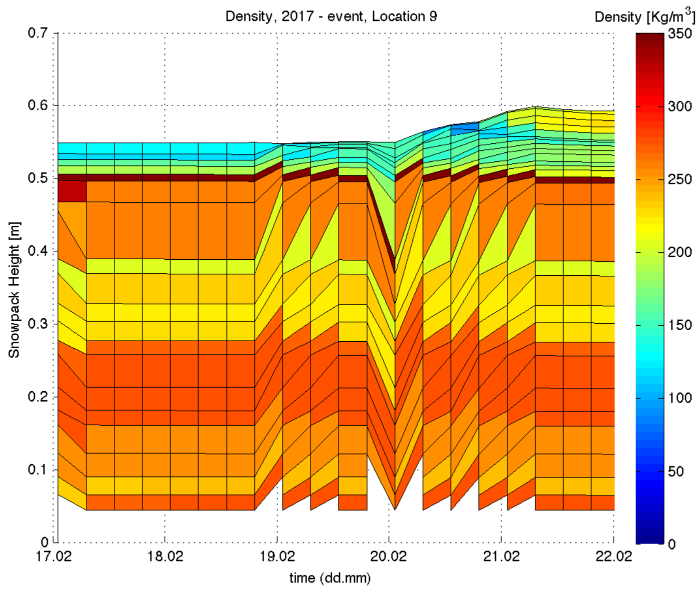

Figure 29: Density profile, 2017 event, location 9

The density profile for location 9 doesn't display any notable horizontal development. The vertical density distribution however, reflects an alternating pattern. A tremendously dense layer in red follows where the relatively light layer at the top of the snowpack. After this initial increase there is a not so dramatic alternating between more and less dense layers. With a notably less dense layer sandwiched between two denser ones at 30 cm. There is also observed another less dense layer, relatively, at 15 cm.

3.3.8 Liquid Water Content

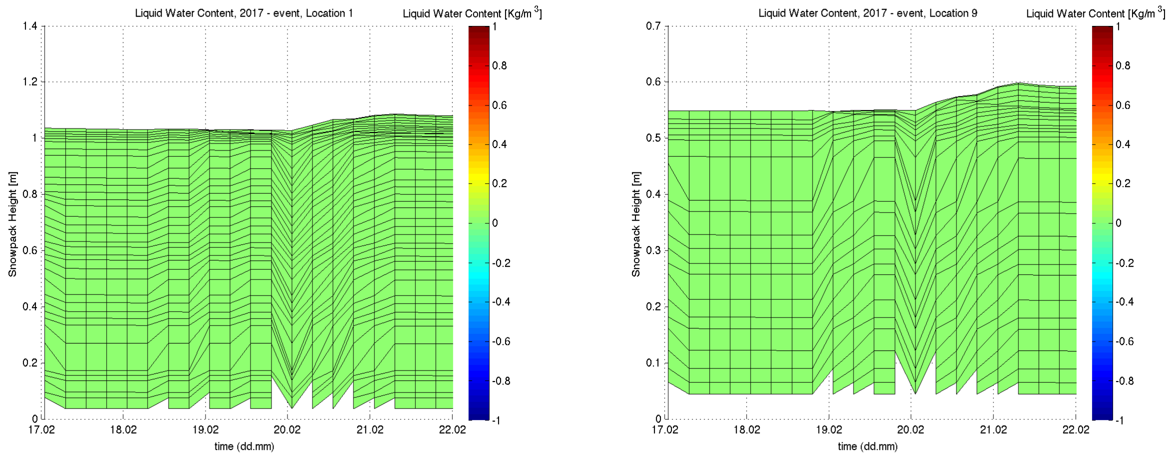

Figure 30: Liquid water content, 2017 event, location 1 and 9

Figure 30 displays liquid water content. The figure clearly displays no liquid water in the snowpack stratigraphy over time. The only notably difference is the one mentioned earlier, which will be the height of the snowpack. Where location 1 through 3 agrees on the height with just over 1 m, and the remaining locations displays a different height profile.

4 Interpretation

This part of the thesis will aim to interpret the quantified results in the light of the quantitative and qualitative methods described in section 2.1 and 2.2, respectively. Generally, the results from two events will be chronologically visited, compared to quantitative field observations when possible, and be evaluated from a snowpack stability perspective. This process will primarily provide crucial insight necessary to address the first research question, concerning the models ability to reproduce internal snowpack conditions and indicate avalanche danger correctly. In addition, this process has the potential to build the foundation to appropriately address all the research questions later. This framework however, carries one exception regarding the variable of liquid water content, which will be visited detached from the remaining interpretation. Now, that the framework of the impendent interpretation are established, the process can commence in an appropriate manner.

4.1 Liquid Water Content

In the interest of realizing a section not repeating itself, some general conclusions applicable to all simulations are necessary. It was found that the variable of liquid water content possessed certain properties, consequently leading to the conclusion of no further consideration of this variable. An explanation for this are provided by Figures 14 and 30 visualizing liquid water content in relation to the 2015 and 2017 event, respectively. The visualization of this variable reveals virtually no liquid water in the snowpack, with the exception of location 1, in 2015. Nevertheless, this snowpack only contains small amounts of water at the bottom, which cannot be considered from an avalanche danger assessment perspective. Now, that the general allegation of no liquid water content in the snowpack at the relevant time step is established the consequences have to be considered: According to McClung & Schaerer (1993) liquid water content influences snowpack stability only when it is present and hence, is of no importance when it is no-existing. Furthermore, Schweizer & Wiesinger (2001) claims that liquid water content influences stability only when the snowpack is not isothermal. Looking at Figures 9 and 21 visualizing a very much existing temperature gradient for all time steps mathematically proves that the snowpack aren’t isothermal. And further implies that liquid water content should be considered, if present. However, as already established the conditions are considered dry, and therefore the temperature gradient perspective can't be applicable. These arguments all points to the fact that, liquid water content and its impact on snowpack stability should not, and will not be further considered in this thesis. This statement and reasoning holds for both the 2015 and 2017 event.

4.2 2015 Event, First Simulation

In contrast to the liquid water content who will not be further considered in this interpretation, there are several other important variables that needs to be evaluated. The arguably most fundamental one concerns Figure 7b visualizing the simulated snowpack thickness for all nine adjacent points leading up to the 2015 event. Comparing the quantified results to the measurements from the DSB report (2016) will undoubtedly reveal a uniformly unsatisfactory simulation of snow depth from this period. The simulation only uncovers 10 cm of snow, whereas the observed fracture line at the site where 2 – 3 m high. There are several challenges with this observation. Firstly, it is the obvious controversy between the model and reality, which arguably influences the credibility of the model in a negative perspective. Furthermore, according to McClung & Schaerer (1993) an evaluation of snow depth is of upmost importance when assessing avalanche danger. If there is insufficient amounts snow in the avalanche starting zone and track to cover terrain and vegetation anchors, and reduce surface roughness features the avalanche danger is no existent. Which leads to the core challenge of the simulation. That a 10 cm snow cover indisputable are insufficient and don't represent any avalanche danger in addition to the model being in controversy with the observations. Because of an conclusively underrepresented volume of accumulated snow and furthermore no imminent avalanche danger, the interpretation will henceforward focus on general signs of instability in regard to increased snow depth and stratigraphy.

Even though the model doesn't successfully simulate general snow depth with acceptable accuracy, the model catches the tremendous overnight increase in snow depth the night leading up to the event. Figure 7b actually quantifies an overnight increase in snow depth ranging from 225 % to 528 % at locations 1 and 7, respectively. This quantification nicely coincides with the qualitative observations of significantly deeper snow covers in the morning hours of 19.02 portrayed in the DSB report (2016). Furthermore an immense short-term increase in snow depth can intuitively represent an increased avalanche danger element. Because the newly accumulated snow represents additional weight to a potential weak layer. This transpiration of events should therefore subjectively alarm avalanche danger forecasters.

If these quantifications are further combined with the temperature profile and gradient from Figures 8 and 9, respectively, a more convincing argument in favor of why this rapid increase in depth should be of concern can be built. These figures reveal a steep temperature gradient in the days prior to the event. Most important from 15.12 – 18.12. However, it should be mentioned that the steep temperature gradient might be a consequence of the underrepresented snow depth in general. Nevertheless, putting these accusations aside, McClung & Schaerer (1993) claims that these conditions in general are unfavorable because it causes snow to loose strength with facet formation. In addition, the approximate temperature gradient in the relevant time step are calculated to be exceeding 100 °C m^{-1}. Which is way above the threshold proposed by Brun, David, Sudul and Brunot (1992), which causes facet formation in the simulated snowpack. This assumption is further fortified in Figure 10, which visualizes facet formation throughout the entire snowpack in correlation with the cold temperatures, and steep gradients of Figure 8 and Figure 9. At this point the situation reflects one where weak bonds are created in the snowpack, followed by a 2 – 5 times depth increase overnight, which represents additional weight to these weak bonds. Lastly, this additional weight is quantified in Figure 13, which shows a shallow, light snowpack transitioning into a much bigger, denser, and hence heavier snowpack. The tremendous amount of weight that is applied to the rounded grain and facet layer (RG+FC) up until the event is therefore quantified in correspondence with McClung & Schaerer (1993) claiming that density profiles can be utilized to calculate the weight on a specific layer. When considering these observations from an avalanche danger assessment perspective, it should undoubtedly raise some concerns already in the very first stages of the interpretation.

Furthermore, considering Figure 11, an initial interpretation will conclude with a favorable grain size distribution. Because the grains are relatively small during the event. This should primarily cause more bonds in between grains, per unit volume and hence increase the stability of the snowpack (Schweizer & Wiesinger, 2001). However, this information should be considered in conjunction with Figure 12 showing ram hardness. This figure overlaps the grain size figure. Whereas a layer of a specific hardness in Figure 12 corresponds to a specific grain size in Figure 11. If this piece of information is considered, one will find relatively low values of hardness, despite small grains in the corresponding layer. Which makes the small grain argument, the only argument somewhat in favor of a stable snowpack to be refuted. Furthermore, Figure 10 showing grain types. Also overlapping with both Figures 11 and 12, reveals that all these layers, to some degree consists of facets. Facets are elongated grains, which represent low stability and as they form decreases the strength of the snowpack (McClung & Schaerer, 1993). This will satisfactory, fully explain why the primarily favorable grain size distribution argument are rejected in terms of assessing the final stability of the snowpack.

In conclusion considering the 2015 event, the model clearly visualizes a dangerous environment. However, because the snowpack thickness is insufficient, there is no distinct stratigraphy to be identified. This situation makes it impossible to predict where the propagation in the snowpack is going to take place, identify any potential slab and, furthermore being qualitatively able to predict the size of a potential event. Also, as earlier mentioned, the snow depth is crucial when forecasting potential avalanche events (McClung & Schaerer, 1993). Meaning, in conclusion, that for the 2015 event the model successfully simulates a dangerous situation. However, the depth is clearly inadequate, causing a diffuse stratigraphy where ultimately no clear forecasting conclusion can be established. Therefore there is clearly need for an additional simulation with increased snowfall to compensate for the existing issues.

4.3 2015 Event, Second Simulation

One of the purposes regarding the second simulation of the 2015 event is to conduct a sensitivity analysis. A sensitivity analysis mainly examines the robustness of the results, by changing the assumptions under which the research is governed in the primary instance (Chin & Lee , 2008). Which is exactly what is achieved when increasing precipitation with a specific factor to reach a superior approximation of the prevailing conditions. However, when performing this undertaking it became imminent that there was not necessary to visualize the corresponding abundance of results to reach a satisfactory, yet precise conclusion. Apart from this, no further justification involving the absence of visualization in regard to certain variables are necessary. Furthermore, this section will interpret the results regarding the second simulation of the 2015 event within the same framework proposed previously.

Firstly, Figure 15 demonstrates how the snowpack thickness differentiates as a function of precipitation, providing two additional scenarios. Specifically, when precipitation are increased with a factor ten or twenty. In this section, these results will not be receiving a great deal of attention. What is noteworthy, however, is to observe that when precipitation increases twentyfold the result is in greater compliance with the observations. As the DSB report (2016) manifests an observed fracture line after the event ranging from 2 – 3 m. This observation, justifies the decision to from here on solely be attentive to the results reflecting the twentyfold increase in precipitation and eliminate the additional scenario from further interpretation.

Furthermore, Figure 17 visualizes grain types when precipitation is increased twentyfold. Noteworthy in this figure is the conspicuous composition of grains in regard to the major precipitation event. Consisting of decomposed, fragmented and rounded grains (DF+RG) as opposed to precipitation particles (PP). A feasible explanation for this concerns the program workflow. If wind speeds exceed a certain threshold for a specific grain type the model assumes that snowdrift occur. Which further induce an increase in snow density and a change of its crystals (Brun, Martin, & Spiridonov, 1997). During this process the model successfully demonstrates that, it do consider snowflakes breaking upon collision with each other and the surface during strong wind condition (Sato, Kosugi, Mochizuki, & Nemoto, 2008), resulting in the distinct composition observed. However, these particles are visualized due to collision between snowflakes inside the relevant grid, and not as a consequence of collision occurring during transport. Therefore, it is important to emphasize that these results, demonstrating both realistic grain types and thickness are not a consequence of CROCUS simulating realistic conditions, but due to artificial forcing. Nevertheless, this approach seems to have overcome the recurrent issue where the model underestimates snowpack thickness as a consequence of not accounting for redistribution by wind. In addition, the figure visualizes something that in this stage of the interpretation can resemble a slab, where the DF+RG layer transitions into a mixture of other grain types. Furthermore, the size of this potential slab is nearly 2 m in thickness, reflecting a more satisfactory situation in agreement with the observed situation (DSB, 2016).

Next, Figures 16 and 18 are subject for interpretation. Visualizing temperature and density, respectively. These are subjected simultaneously in consideration of them being dependent, according to equation (1) from Vionnet et al. (2012). Analogous to the primary simulation, the in comparison cold and soft snowpack abruptly transitions into a colossal, warm and dense snowpack. According to Schweizer and Wiesinger (2001), dense and warm snow on top of loose, cold snow is unfavorable. These specific conditions are reflected in the respective figures at the relevant time step, causing a disadvantageous situation in relation to stability. Furthermore, according to McClung & Schaerer (1993) does density and hardness correlate. Whereas, hardness decreases as density decreases, and conversely. In addition, density stratigraphy can determine the weight and force applied to a certain layer (IBID). Therefore the stratigraphy in Figure 18 is extremely concerning, whereas a less dense and presumably weaker layer are located underneath more than 1 m of denser snow, in comparison. Furthermore, this transition correlates to the transition concerning grain types from Figure 17, further fortifying the hypothesis of this being a dangerous slab. All of these assumptions imply grave avalanche danger. In addition, to the slab now being a respectable size, capable of representing a hazard (IBID) and correlating with the observed fracture line (DSB, 2016).

Furthermore, looking at Figures 16, 17 and 18, visualizing temperature, grain types and density, respectively, in regard to the second simulation of the 2015 event. A premature conclusion could have occurred in this comparison, concerning the primary increase in snowpack thickness at 13.12. Because the increased thickness is of notable size, avalanche danger could have been imminent. However, the difference between the two precipitation events of which increased the snowpack thickness is not the increase solely. Rather under which conditions the increase occur. The primary increase not only consists of other grain types, which in this instance is of relatively low importance, compared to the temperature and density regime the increase occurs under. In comparison does the second increase occur under fundamental different conditions, where the snowpack are notably both warmer and denser. In addition to a slab-like structure occurring in both Figure 18 and Figure 17 provides foundation for concluding with avalanche danger at the correct time interval, and not in relation to another, adjacent precipitation event.

Conclusively, from an avalanche danger assessment point of view, the new, modified results in regard to the 2015 event are satisfactory. Now successfully simulating sufficient amounts of snow, in addition to a slab-like structure and an allover unfortunate stratigraphy in regard to the remaining variables. Therefore, from an avalanche danger assessment and forecasting point of view, the results are post modifications, deemed satisfactory, and furthermore reflecting a better approximation of the observed conditions and in addition prevailing avalanche danger at the correct time step.

4.4 2017 Event

Concerning the interpretation of the 2017 event, a short introduction to the framework the argument will work within is beneficial. Firstly, two figures will be considered in most instances. An interpretation of Figure 19b, showing snowpack thickness profiles provides an explanation for this decision. There are recognized two general thickness trends for all locations, at approximately 1 and 0.6 meters. Whereas the former consists of location 1, 2 and 3 (Fig. 19b), which all are located at significantly greater elevations in comparison to the remaining locations (Table 1). Vikhamar-Schuler, Müller and Engen-Skaugen (2011) found that simulated snowpack thickness were the most sensitive to differences regarding precipitation and air temperature input. These variables differentiate with elevation (Marshall & Plumb, 2008: DeWalle & Rango, 2008) and consequently two thickness trends occurred. Because temperature and precipitation input influence a considerable amount of output data within the snow cover model CROCUS (Vionnet et al., 2012), this phenomenon was likewise observed concerning the remaining variables. Which is why two figures have to be considered in the interest of an expedient interpretation. Furthermore, one day prior to the avalanche event itself, NVE recorded a snowpit and conducted an extended column test, in the same slope of which the event later took place. The results from these undertakings are available within their report summarizing the event (Landrø, Mikkelsen & Jaedicke, 2017), and will further be used as a corrective tool when interpreting the accuracy of the model. Therefore, the interpretation will primarily consider the output of the model in relation to snowpack stability theory, and further utilize the field measurements to evaluate the accuracy of the model. Now, that the premises of which the interpretation will be based on are established, it can commence.

According to McClung & Schaerer (1993) is the most fundamental part of assessing avalanche danger an evaluation of snowpack thickness. Aiming to elucidate whether there are sufficient amounts of snow to represent a hazard. As previously mentioned does two conspicuous thickness trends regarding thickness occur. Approximately between 0.6 and 1 meter (Fig. 19b). Comparing the two trends undoubtedly reveals that the latter trend represents a much greater hazard than the former although both amounts would be sufficient to cause a destructive event. However, when comparing the output of the model to relevant field measurements, manifesting a recorded snow depth of 1.25 m one day prior to the event (Landrø, Mikkelsen, & Jaedicke, 2017), the imminent conclusion is that the latter trend superiorly describes the prevailing conditions. In addition to this conclusion would an analysis of the discrepancy between the two trends be beneficial to provide an explanation for this interpretation: As concluded does the discrepancy occur due to the fact that the locations represented by a certain trend are located in different elevation bands. Namely are location 1, 2 and 3, located at 401, 311, and 329 m a.s.l., respectively, much closer to the top of Sukkertoppen, being located at 371 m a.s.l. (Bolstad & Barr, 2017). Therefore, the meteorological conditions at these locations are superiorly analogous to the ones at the site of the event. Durand, Giraud, Brun Mérindol and Martin (1999) concluded that this is one of the assumptions under which the model has to be utilized. Claiming that areas within the same region with similar aspect and elevation produce analogous conditions. Therefore, the tentative conclusion is that the simulation of location 1, 2 and 3 makes a superior approximation to the prevailing conditions in the relevant area.

Figure 21 and Figure 20 display temperature gradients and profile, respectively. The temperature trends are assumed to be identical, regardless of snow depth. Therefore, the following argument holds for all simulated locations in regard to these variables in 2017. Firstly, Figure 21 reveals that all temperature gradients are exceeding the models threshold of 5 °C m^{-1}, causing the model to favor the evolution of facets (Brun, David, Sudul, & Brunot, 1992). In addition to the models quantification a qualitative description concerning the horizontal temperature evolution can provide a more nuanced argument. Figure 20 visualizes, in the time interval from 05.02 – 12.02, a close to isothermal snowpack approaching the melting point. This warm snowpack then abruptly transitions into a tremendously cold one, resulting in unfavorable conditions from a stability point of view. Such temperature fluctuations consequently lead to formation of facets at the surface, which represents a weak layer with the potential for burial (Landrø, Mikkelsen, & Jaedicke, 2017). Nevertheless, what argument one is the most inclined to utilize, the model does simulate the conditions accordingly. Quantified in Figures 22 and 23 displaying grain type distribution at location 1 and 9, respectively, reveal buried facets in an abundance of layers. In relation to burial of weak layers, one day prior to the event, NVE observed an increased snowpack thickness at Svalbard Airport of 15 cm (IBID). Only the figures representing the trend of locations 1, 2 and 3 manage to reproduce this distinct increase. Therefore, the tentative conclusion of this trend being superior still holds. Nevertheless, accuracy in relation to observations aside, both trends simulates satisfactory unstable conditions.

One day, prior to the destructive avalanche event there were performed an extended column test in the same area as the avalanches were later triggered (Fig. 31). This is of great interest when interpreting the output of CROCUS, because the extended column test give explicit data on where the weak layers are located and hence can work as a corrective comparison tool in this process. Figure 31 nicely coincides with the top 25 cm of Figure 22 showing grain types for location 1, and Figure 26 showing ram hardness for location 3. One have to keep in mind that the comparison have to be somewhat liberal, but accusations and setbacks aside the weak layer in question considering the snowpit from the NVE report should be around the 0.8 mark in the figures representing the assumed superior trend. Further, looking at Figure 24 and 28 displaying grain size and density, respectively, characteristic weak features coincide with the propagation height from the extended column test NVE conducted prior to the event. Where a

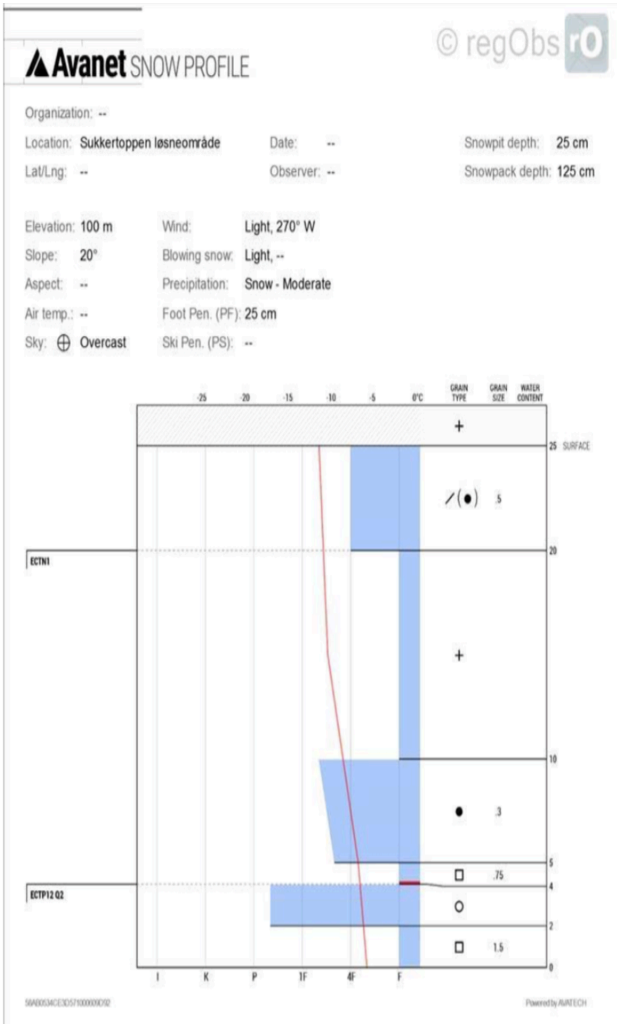

Figure 31: Snow profile, included extended column test from the same slope as the destructive event later took place (Landrø, Mikkelsen & Jaedicke, 2017)

layer of notably less dense snow, and significantly greater grain sizes correlates to the weak layer from the stability test. Furthermore, considering Figures 22 and 26 visualizing grain types and hardness, respectively, displays an unfavorable stratigraphy. Where primarily facets are located in this area, in conjunction with a significantly softer layer. All abovementioned variables conclusively display weak features at the same height as the propagation from the extended column test displayed in Figure 31. Therefore the model is conclusively, satisfyingly accurate simulating the top layers and further the propagation of the event itself considering the 2017 event. It should be mentioned, however, that this argument only holds for the already suspected most accurate trend of location 1, 2 and 3. The results from the remaining locations are in need of another interpretation, as they don't correlate with the recorded snowpit in neither depth nor stratigraphy. For that reason only general signs of instability will be considered, in relation to the output of the model.

Considering the secondary trend, tremendous avalanche danger is simulated, despite inadequate correlation to the field observations. First of all, the visualized grain types in Figure 23 displays an exclusively unfavorable stratigraphy. Where there are no traces of theoretically stable grain types such as rounded grains, instead the snowpack consists of grain types such as facets and depth hoar. Very notably is the distinct transition of grain types into exclusively depth hoar in the layer ranging from roughly 0.2 – 0.4 m. This transition coincides with the increase in snow depth prior to the triggering of the event, although it doesn't reproduce the correct amounts (Landrø, Mikkelsen, & Jaedicke, 2017). Furthermore, the horizontal evolution of several variables such as grain size (Fig. 25) and ram hardness (Fig. 27) accompanying the depth increase points to worrisome conditions. Abrupt increases in grain sizes and sudden decrease in hardness right before the event, in combination with the precipitation event are all clear signs of an unstable snowpack emerging. In addition, Figure 29 showing density throughout the snowpack over time visualizes a persistent weak layer at 0.3 – 0.4 m, which also coincides depth-wise with all the other abovementioned signs of instability. Even though, this second trend doesn't correlate with the observation in this specific slope, the model successfully simulates unstable conditions in the area. It should also be mentioned, that the weak layers identified in the second trend all shows instability signs at the same distance from the surface, which directly correlate to the distance from the surface the propagation took place in the extended column test. One can speculate in whether these layers correlate, but since the snowpack in general displays significant differences to the snowpit of NVE this will all be classified as speculations.

In conclusion, the model simulates the conditions and consequently the avalanche danger with great accuracy. Although, all locations didn't feature a satisfactory correlation with the quantitative observations, they did indicate avalanche danger at the correct time step. Which is the most fundamental concern regarding the utility of CROCUS as an avalanche danger forecasting tool in the region. Therefore, provided that the methods of Durand, Giraud, Brun, Mérindol and Martin (1999) are accounted for, the model does provide satisfactory results regarding the scope of this thesis.

5 Discussion

This part of the thesis will aim to discuss the findings and their significance in relation to the scope and research questions presented in section 1.2. Prior to this conclusive subsection several affairs need to be sorted, in order to appropriately comment on the research questions. These include a sensitivity analysis in regard to the second simulation of the 2015 event, and error sources and the magnitude of which they impact the credibility of the results. After sorting the significance of these influences, the research questions can be addressed. Namely, the models ability to reproduce observed conditions, an evaluation of AROME-Arctic as forcing, and a investigation of how the findings in this study can assist future forecasters.

5.1 Sensitivity Analysis

Previously, the interpretation concerning the second simulation in regard to the 2015 event was justified with an upcoming sensitivity analysis. In that respect, this section will aim to conduct the promised sensitivity analysis based on the results and interpretation of the second simulation. A Sensitivity analysis can also be defined as a study of the relative importance of different input factors on the model output (Saltelli, 2017). Knowledge concerning the range of uncertainty different variables imposes on the results, can clarify the extension of the study and furthermore contribute to the assessment of the model. In such a context, the purpose of this section is to discuss the relative importance of precipitation as a variable in the model, and how the conclusions from this analysis have implications on the scope of the thesis.

5.1.1 Sensitivities Regarding Snowpack Thickness

The first part of the sensitivity analysis will aim to diagnose how snowpack thickness in Figure 15 differentiate when precipitation are increased with a specific factor. For this analysis to be conducted appropriately, it is expedient to notice that there are two precipitation events recognized. This section will refer to the precipitation event from 12.12 – 15.12 as the first precipitation event, and the precipitation event leading up to the avalanche event as the second precipitation event. In that regard, two peculiarities are recognized. The first one concerns that although precipitation relative to the original scenario remains constant, the corresponding thicknesses differentiate. The second peculiarity recognizes differences in thickness within specific precipitation events.

Firstly, it is observed that even though the increased precipitation factor remains constant throughout the visualized period in Figure 15 for all scenarios, the observed snowpack thicknesses don't differentiate correspondingly. Figure 15 demonstrates a smaller increase in snowpack thickness during the first precipitation event compared to the second for both additional scenarios. A key difference between the two precipitation events is the conditions under which they occur. During the second precipitation event are temperature and wind speeds much greater in comparison with the first (Yr, 2015a: Yr, 2015b: Yr, 2015c). These variables influence the density of snowfall, whereas equation (1) dictates if T_a and U increases, ρ_{new} increases. This density value is used to convert precipitation amount into thickness (Vionnet et al., 2012). Figure 18 demonstrates this quantification, visualizing greater densities during the second precipitation event compared to the first. Therefore, snowpack thickness doesn't differentiate solely as a function of precipitation. Additionally it differentiates as a function of the prevailing conditions under which the precipitation occur.

Secondly, it is observed that during the second precipitation event the twentyfold increase in precipitation are twice the size of the tenfold increased. And, during the first precipitation event the twentyfold increase in precipitation are four times greater than the tenfold increase. This is peculiar, because the conditions governing each precipitation event are identical. Therefore, general intuition states that the factor between the additional scenarios should remain identical throughout the relevant period. This is clearly not the case, presumably because the factor of which precipitation increase differentiates. Equation (5) dictates that if σ increases, which it does with increased precipitation, the compaction increases (Vionnet et al., 2012). Therefore, during the second precipitation event, where more snow accumulates (DSB, 2016), the compaction increases, resulting in smaller differences between the scenarios during the second precipitation event. Therefore, snowpack thickness and its evolution is conclusively a complicated system, having to take a myriad of variables into account to accurately simulate natural conditions. Additional quantitative analysis of this system will not be considered in this thesis, because it would violate the scope of the thesis.

5.1.2 Implications of The Sensitivity Analysis

Considering the quantification of uncertainty, specifically the models need to increase precipitation twentyfold in order to simulate satisfactory thickness (Fig. 15) is interesting. This aspect proves the models immense range of uncertainty outside its place of origin, and eliminates long-term avalanche forecasting from the models possible applications in Svalbard. Because in a hypothetical scenario, were a potential forecaster aims to forecast avalanche danger three days from a random point in time, which is the range of AROME-Arctics forecasts (Met.no, 2018), its feasible that the thickness of the simulated snowpack needs to increase several times in order to reflect a realistic situation at the desirable time. In addition, the model relies on an accurate weather forecast to work properly as an avalanche danger forecasting tool. Adding the necessity to take into account the uncertainty in potential weather forecasts when assessing the uncertainties in the model. The range of uncertainty is simply to substantial for long-term applications to be reasonable.

On a short-term scale, the models applications are more relevant from a forecasting perspective as a consequence of the models need to increase precipitation twentyfold to reproduce the prevailing snowpack conditions. If a potential forecaster attempts to assess stability one day from a random point in time, the weather forecast in relation to model output can help a forecaster to qualitatively consider adjusting the models input to reach a realistic output. This is however a qualitative consideration, which relies on the potential forecasters experience and ability to assess a models output in comparison to the forecasted conditions. In that regard, the potential forecaster need to take into account the previously discussed sensitivities, whereas the snowpack thickness is sensitive to conditions, in addition to not increasing linearly, but compacting under its own weight. Due to all these uncertainties, especially in relation to the model not taking redistribution by wind into account (Vionnet, et al., 2012), at this stage, the models applications extend, solely to supplement current forecasting routines. This is a consequence of the issue concerning that the model had to be run more than once to reflect realistic conditions. Therefore, to increase the models potential application in the area, this issue needs to be resolved.

5.2 Error Sources and Limitations

An analysis of plausible error sources and the magnitude of which they impact the credibility of the results are always beneficial. Such an analysis will intuitively contribute to a broader understanding of the extension of the thesis. Furthermore, understanding how different uncertainties impact the output of the model are essential to produce valuable comments on the research questions later. The investigation of the error sources will include representativeness of points, and in that regard how snowpacks representative for a broader region have been selected. Thereafter, internal error sources concerning the program workflow will be analyzed. Following will a note on how the prevailing conditions limit the conclusion and additional universal limitations be discussed. All these aspects have the potential to provide important insight essential to make relevant comments on the research questions later in this section.

5.2.1 Representativeness of Points

When collecting data in a region, different locations produce different statistics. As a result, selecting specific locations to represent the prevailing conditions can be a significant challenge (DeWalle & Rango, 2008: Temper, 2008). Therefore, an analysis of this issue have the potential to help potential future forecasters better manage the model as an avalanche danger assessment tool.

Precipitation and air temperature are pivotal input data, influencing a considerable amount of the output within the snow cover model CROCUS (Vionnet, et al., 2012). These variables differentiate with elevation (Marshall & Plumb, 2008: DeWalle & Rango, 2008), consequently causing snowpacks within a region to present similar features at similar elevations on slopes of similar aspect (Durand, Giraud, Brun, Mérindol , & Martin, 1999). Because Arome-Arctic operates with a 2.5 km grid (Met.no, 2018), the spatial distribution of the forcing points produce different elevations for each individual point. This issue is illustrated in Figure 7a and Figure 19a demonstrating snowpack thickness for all locations in the winter season of 2015/2016 and 2016/2017, respectively. The figures reveal tremendous dissonance between locations solidifying the challenge proposed. Location 1, 2 and 3, however, are all located at somewhat corresponding elevations to the release area (Table 1), but yet cannot be directly applied to represent the prevailing conditions. Because aspect is not considered in the forcing, but influences the evolution of a snowpack in natural conditions (Durand, Giraud, Brun, Mérindol , & Martin, 1999), the model output from these locations possesses potential errors. Therefore, representative output are selected based on the findings of Durand, Giraud, Brun, Mérindol and Martin (1999), claiming that it is possible to simulate main characteristics of the snowpack in a given region provided a sufficient amount of snowpacks are simulated, on different elevations. From here persistent main characteristics present in the vast majority of simulated snowpacks, can be identified, and furthermore be utilized to represent snowpack conditions in a broader region.

That said, Figure 7a and Figure 7b reveal satisfying coherence between locations regarding thickness during the relevant time step. This coherence translates into the remaining variables. Because all nine forcing points present similar results, the potential challenge regarding representativeness of points falls. Furthermore regarding the 2017 event, a real-time stability test in addition to a snow profile is accessible and can potentially correct the results and the best-approximated simulation can be utilized. Conclusively, in this thesis the model was either in great compliance with itself or comparative corrective tools existed, which made it possible to choose the best approximation. Representativeness of points is therefore not an issue with significant clout, concerning these events specifically, but is however a recurrent issue concerning the nature of this kind of research.

5.2.2 Internal Error Sources

Durand, Giraud, Brun, Mérindol and Martin (1999) found some significant internal limitations in regard to the program workflow. These concern the cumulative effect of all daily errors throughout the season not having any direct correctional possibility and the issue of snow redistribution by wind not being accounted for in the model. Every one of these limitations was observed in this study, leading to potential inaccuracies and limitations regarding the study in its entirety. Therefore will this subsection aim to describe how these issues influenced the output of model.

As previously mentioned was CROCUS primarily tested in the French Alps, which is a region where snow redistribution by wind primarily doesn't influence the snowpack conditions with the same magnitude (Brun, David, Sudul, & Brunot, 1992). This is however of paramount importance at Svalbard where some areas might be covered in several meters of snow, while others are completely blown free (Eckerstorfer, 2013). Regarding the 2015 event, the model wasn't remotely able to recreate the amounts of snow and consequently failed to simulate a trustworthy stratigraphy. In addition, did the DSB report (2016) credit the horrendous amounts of snow to the redistribution, and hence a fundamental challenge regarding the utility of CROCUS in Svalbard arises. Therefore, when the model doesn't take the magnitude of such a process into account, the error cumulates throughout the season and culminates at decisively underestimated snowpack thicknesses. Consequently, both internal limitations from Durand, Giraud, Brun, Mérindol and Martin (1999) are observed. Nevertheless this issue wasn't completely recurrent in the 2017 event where the snow depth was satisfactory recreated at some locations.

The issue however, was anticipated and therefore a hypothesis concerning this specific error source was presented in section 1.1. Furthermore, a possibility to resolve the issue within the framework of the thesis was achievable because correctional data concerning snowpack thickness existed. Nevertheless, in a no-play situation, this possibility might not be existent, and therefore conducting a realistic correctional process represents a formidable challenge, where the governing factors discussed within the sensitivity analysis have to be accounted for. In section 5.1.2 the implications of this limitation are discussed. Due to the structure of the thesis an elaboration of the solution to this problem within the current model system will not be presented in this section. However, in both events, the model successfully simulated dangerous conditions at the right time step. So even though the model, in most cases didn't manage to recreate the conditions with 100% accuracy it still managed to provide what would have been valuable information to potential forecasters. Nevertheless this is a reemerging issue that one gravely recommends to solve prior to implementing this model in avalanche forecasting at Svalbard. Mainly to raise the models credibility to acceptable levels, due to the tremendous responsibility resting on forecasters shoulders.

5.2.3 Limitations Concerning Conditions

Snowpack metamorphism processes vary between dry and wet snow (DeWalle & Rango, 2008). Because section 4.1 classified all snowpacks regarding this thesis as dry, it raises prevailing issues regarding the extension of the thesis, which needs to be addressed. Intuitively, it follows that none of the conclusions solidified in this thesis applies to wet conditions, which consequently leads to significantly fewer applications in comparison with the ambitions of the thesis. Therefore, this subsection will describe analogous work, in an attempt to clarify the situation.

Some light can be shed on the situation from previous work, whereas numerical models have been utilized to assess avalanche danger when conditions are classified as wet. Another numerical model calculating the internal evolution of a snowpack as a function of energy mass-transfer between the snowpack and the atmosphere is SNOWPACK (Lehning, Bartelt, Brown, Russi, Stöckli, & Zimmerli, 1999). This model is analogous to CROCUS and can henceforward be used to discuss the models expected performance. In Norway, Jordet (2017) assessed the performance of SNOWPACK in wet conditions. He found that the numerical model simulated the internal state of the snow cover accurately, provided sufficiently dense forcing data. Since the density of forcing data is a non-existent issue concerning the method of this thesis, it is plausible that CROCUS also could simulate wet conditions, in Norway, with satisfactory accuracy. Because this assumption is based on a comparison between two numerical models and therefore is thought analogous, it is only speculations. Nevertheless speculations that have to be considered in the interest of potentially expand the extension of this study.

5.2.4 Universal Limitations

A paramount observation concerning the extension to the findings of this study, affecting all conclusions made prior and after this subsection involves their transferal value to alternative regions. Section 5.1.3, conclusively state that the inferences from this study only holds for dry conditions, because all simulated snowpacks demonstrate dry conditions. Furthermore, two revisited events are a definite insufficient premise on which to make universal conclusions. Therefore, due to limitations as a consequence of conditions and concerning sparse observations the transferal value of the study to arbitrary regions is associated with uncertainties. Consequently, additional research is necessary prior to implementing the model in both the relevant and alternative regions.

5.3 Research Questions Revisited

This subsection will aim the address the research questions from section 1.2 based on the findings in this study. In that regard, an understanding off the framework governing the discussion is beneficial. Firstly, the question concerning the models ability to reproduce snowpack stratigraphy in Longyearbyen, Svalbard will be addressed. Furthermore, an evaluation of the external insecurities, specifically forcing will be addressed. Primarily aiming to evaluate whether the forecasting model of AROME-Arctic provides sufficient input. Finally, an investigation of how the model system can support future forecasters in their stability assessments will be addressed.

5.3.1 Ability to Reproduce Snowpack Stratigraphy

First, an analysis of whether the model successfully managed to reproduce the snowpack stratigraphy, and therefore avalanche danger at the correct time step is imminent. Because there were no organized forms of avalanche danger assessment in the region, until after the 2015 event (Landrø, Mikkelsen, & Jaedicke, 2017), the assessment will differentiate regarding the two events. Depending on whether quantitative observations existed.

The models ability to reproduce snowpack stratigraphy in regard to the 2015 is a complicated one, mainly because few quantitative field observations exist. However, if the observed thickness is compared to the simulated thickness in conjunction with the stability assessment of the simulated snowpack a conclusion can be reached. In the instance of the first simulation, the results are undoubtedly inaccurate due to the immense discrepancy between observed and simulated thickness. As previously discussed, this issue and its range of insecurity leads to a conclusive inability to forecast long-term avalanche danger. Therefore, concerning the timescale of hours or maybe even days, potential forecasters have to keep in mind that the model might need reasonable forcing to reach a satisfactory approximation of the prevailing conditions. This means that if the model simulates wildly underestimated amounts of snow, which don't translate into the conditions observed outside, the forecasters should consider forcing the model with additional precipitation. If this is successfully accomplished, the model would very much be able to reproduce the conditions, and therefore forecast the 2015 event with acceptable accuracy. However, it should be noted that the 2015 event feature a distinct occurrence of events, which displays significant avalanche danger, in addition to no-existing quantitative observation. Therefore, the model doesn't encounter unmanageable demands concerning the reproduction of conditions in this instance. Consequently, the questions on the models ability to reproduce the prevailing conditions require additional research and examples.

Furthermore, in the interest of investigating the accuracy of the 2017 event, quantifiable observations exist. These observations can further be utilized as corrective tools concerning this assessment. In this instance, the model displayed great ability to reproduce the observed stratigraphy. Whereas model output, produced an overlapping stratigraphy in regard to the observed. These are conclusively satisfactory accurate results concerning this aspect of the study. However, there are some challenges in regard to the models ability reproducing avalanche danger, which needs to be addressed. Prevailing conditions and avalanche danger level are dependent variables (Temper, 2008: Buser, Föhn, Good, Gubler, & Salm, 1985). However, in this specific instance these variables did not posess a traditional correlation, consequently leading to the model being incapable of comprohending the transpiration of events. This transpiration included the ultimately harmfull event being triggered by the settling of another avalanche originating further uphil (Landrø, Mikkelsen, & Jaedicke, 2017). Reproducing such conditions is beyond the ability of the model. However, assessing avalanche danger for a specific slope is unreasonable and not in unison with existing theory (Temper, 2008). The observations in which the model correlates consequently led NVE to assess the prevailing avalanche danger in the region to level four, which is large (Landrø, Mikkelsen, & Jaedicke, 2017). From the satisfactory correlation it follows that forecasters with access to this model would have reach the same conclusion. So Although, the model could never been expected to forecast the specific event, and how it transpired, it was both able to reproduce prevailing conditions and furthermore reflect grave avalanche danger, which is very much satisfactory considering the scope of this thesis. Therefore, based on the findings from these two events, the snow cover model of CROCUS does simulate snowpacks very similar to those observed in the field under dry conditions in Longyearbyen, Svalbard. Provided that the model, naturally or artifically simulates accurate snow depth, regarding the two events in this thesis.

5.3.2 Evaluation of Forcing

Vikhamar-Schuler, Müller and Engen-Skaugen (2011) found that different kinds of forcing impacted the model output. Therefore, an investigation of whether the forcing from AROME-Arctic provides satisfactory results is imminent. In this region, there are three fundamental arguments favoring this kind of forcing, as opposed to the alternative of automatic weather stations. Namely, spatial density, operativeness and forecasting ability.

Firstly, there are only one automaic weather station in the periphery of Longyearbyen, located at Svalbard Airport 3.9 kilometers from the settlement (Yr.no, 2018). On the other hand does AROME-Arctic work with a 2.5 km grid throughout the entire area (Met.no, 2018) (Fig. 5). In the interest of forecasting avalanche danger, the comparison and identification of persistent features at several representative locations provides a superior approximation to the prevailing conditions (Durand, Giraud, Brun, Mérindol , & Martin, 1999). As opposed to the sole point in space that the automatic weather station represents, the forecasting system of AROME-Arctic is conclusively superior regarding spatial density. This argument extends into the remainder of Norway. As Vikhamar-Schuler, Müller and Engen-Skaugen (2011) stresses the drawback concerning the sparse network of automatic weather stations in Norway.

Furthermore, automatic weather stations frequently malfunction, especially in cold climate (Strangeways, 1985). One example of this comes from Schuler, Dunse, Østby and Hagen (2013), which analyzed automatic weather station data over Austfonna in an 8-year period. During this period, the automatic weather station malfunctioned a calculated minimum of 827 days. Although this station are far more remote than the Svalbard Airport station, consequently only being visited annually in the interest of maintenance and restoring data (Schuler, Dunse, Østby, & Hagen, 2013), this argument speaks to the sensitivity of automatic weather stations as opposed to the forecasting model. Nevertheless, the forecasting model of

AROME-Arctic bypasses this disadvantage, yet again favoring this kind of forcing considering the scope of this study.

One advantage, possibly favoring automatic weather stations over forecasting models concerns their exceedingly accurate data. Because automatic weather stations conduct in situ acquisition of data (Schuler, Dunse, Østby, & Hagen, 2013), the acquired data are consequently more accurate. However, the objective of utilizing CROCUS in this instance concerns avalanche forecasting. From this, it intuitively follows that the input data have to represent future conditions, which is the purpose of AROME-Arctic (Met.no, 2018), as opposed to automatic weather stations (Schuler, Dunse, Østby, & Hagen, 2013). This argument favors AROME-Arctic because forecasts provide a more realistic approach to a possible utilization of this model in an avalanche forecasting perspective. Nevertheless, the insecurities concerning accuracy in this study don't seem to be a consequence of forcing, but rather the program workflow. With reference to the redistribution by wind, which was one of the main error sources in this study. When this internal issue was accounted for, the model system simulated snowpacks very similar to those observed in the field. Therefore, the argument of automatic weather stations providing superiorly accurate data, in comparison to AROME-Arctic is refuted. When all these aspects are accounted for, the forecasting model AROME-Arctic provides satisfactory results and seems to be the most beneficial in regard to the possible utilization of this model system in Longyearbyen.

5.3.3 A Numerical Model Assisting Forecasters in Future Work

When investigating how CROCUS can assist future forecasters with stability assessments, two arguments lead to a potential application. Firstly, concerning the 2015 event, the model did manage to reproduce satisfactory stratigraphy, and thickness after artificial forcing. The range of uncertainty concerning this issue has previously been discussed in section 5.1.2, consequently eliminating long-term avalanche danger forecasting from the models potential applications in the region. From the uncertainties regarding accurately simulating these variables it follows that excessive reliance on the models ability in general is premature in the relevant region.

Secondly, the conclusions regarding the model providing satisfactory results in relation to the 2017 would arguably not have been reached if a potential interpreter didn't have access to the stability tests conducted prior to the event. The 2017 event don't feature a distinct change in conditions such as the 2015 event, referring to the incredible increase in snow depth leading up to the avalanche. In contrast, the 2017 event feature more diffuse signs of instability. For that reason, one is arguably in need of the stability testing results to clarify and work as guidelines, and furthermore reach a superiorly trustworthy conclusion. Again, favoring the conclusion of complete dependence on the model being premature.

However, due to the superior time and spatial density of the model, in comparison with traditional methods, in addition to the models satisfactory results regarding ability to reproduce snowpack conditions, it can very much supplement the current methods. Therefore, a hybrid approach has the potential to be beneficial in the future, regarding utilizing CROCUS as an avalanche danger forecasting tool in Longyearbyen. Nevertheless, if the primary issue is resolved, making the model consider redistribution of snow in between grids, the dependence on the model can potentially increase.

6 Conclusion

In this study, the snow cover model of CROCUS have been assessed in the light of two destructive avalanche events transpiring in 2015 and 2017 with forcing from the weather forecast model AROME-Arctic. Three research questions were addressed in section 1.2 to appropriately assess the models performance as a potential tool for avalanche danger forecasting. This section will summarize the findings chronologically.

Firstly, CROCUS simulates satisfactory stratigraphy and consequently reflects avalanche danger at the correct time step in Longyearbyen. However, because the program workflow don't account for redistribution by wind (Vionnet, et al., 2012), uncertainties arise in regard to snow depth estimates, and future utilization of the model in the region. Nevertheless, provided satisfactory simulations of snow depth, artificially or naturally, the model simulates snowpacks very similar to those observed in the field.

Secondly, AROME-Arctic provides satisfactory input data considering the purpose of avalanche danger forecasting. Compared to alternatives such as automatic weather stations, AROME-Arctic possesses a superior density of measurements, it is not prone to malfunctions such as automatic weather stations, and it posses the ability to forecast conditions (Met.no, 2017: Met.no, 2018). This makes it suitable as forcing for CROCUS from the perspective of avalanche danger forecasting the region.

Finally, because of the uncertainties regarding the models ability to reproduce snowpack thickness, and the absence of destructive testing, a complete dependence on the models capability is premature. However, due to the superior time and spatial density of the model, in comparison with traditional methods it can very much supplement the current methods. Therefore, a hybrid approach has the potential to be beneficial in the future, regarding utilizing CROCUS as an avalanche danger forecasting tool in Longyearbyen.

7 References

Bair, E., Simenhois, R., van Herwijnen, A., & Birkeland, K. (2015). Using 2 m Extended Column Tests to Assess Slope Stability. *Cold Regions Science and Technology , 120*, pp. 191-196.

Bolstad, E., & Barr, S. (2017). *Store Norske Leksikon*. Retrieved 4 18, 2018, from Sukkertoppen - Svalbard: https://snl.no/Sukkertoppen_-_Svalbard

Boone, A., & Etchevers, P. (2001). An Intercomparison Of Three Snow Schemes Of Varying Complexity Coupled To The Same Land-Surface Model: Local Scale Evaluation At An Alpine Site. *Journal Of Hydrometeorology , 2* (4), pp. 374-394.

Brun, E., David, P., Sudul, M., & Brunot, G. (1992). A Numerical Model To Simulate Snow-Cover Stratigraphy For Operational Avalanche Forecasting. *Journal Of Glaciology , 38* (128), pp. 13-22.

Brun, E., Martin, E., & Spiridonov, V. (1997). Coupling A Multi-Layered Snow Model With A GCM. *Annals of Galciology , 25*, pp. 66-72.

Brun, E., Martin, E., Simon, V., Gendre, C., & Coleou, C. (1989). An Energy And Mass Model Of Snow Cover Suitable For Operational Avalanche Forecasting. *Journal Of Glaciology , 35* (121), pp. 333-342.

Buser, O., Föhn, P., Good, W., Gubler, H., & Salm, B. (1985). Different methods for the assessment of avalanche danger. *Cold Regions Science and Technology , 10* (3), pp. 199-218.

Chin, R., & Lee , B. (2008). *Principles and Practice of Clinical Trial Medicine.* Academic Press.

Colbeck, S. (1983). Theory of methmorphism of dry snow. *Journal of Geophysical Research , 88* (C9), pp. 5475-5482.

Colbeck, S. (1980). Thermodynamics of snow metamorphism due to variations in curvature. *Journal of Glaciology , 26* (94), pp. 291-301.

Cuffey, K., & Paterson, W. (2010). *The Physics Of Glaciers* (4. edition ed.). Burlington, Massachusetts, USA: Elsevier.

deQuervain, M., & Meister, R. (1987). 50 years of snow profiles on the Weussfluhjoch and relations to the surrounding avalanche activity (1936/37-1985/86). *IAHS Publications , 162*, pp. 161-181.

DeWalle, D., & Rango, A. (2008). *Principles of Snow Hydrology.* Cambridge University Press.

Dickson, R., Osborn, T., Hurrell, J., Meincke, J., Blindheim, J., Adlandsvik, B., et al. (2000). The Arctic ocean response to the North Atlatnic Oscillation. *Journal of Climate , 13*, pp. 2671-2696.

DSB. (2016). *Skredulykken i Longyearbyen 19. desember 2015.* Direktoratet for samfunssikkerhet og beredskap (DSB).

Durand, D., Giraud, G., Brun, E., Mérindol , L., & Martin, E. (1999). A computer-based system simulating snowpack structures as a tool for regional avalanche forecasting. *Journal of Glaciology , 45* (151), pp. 469-484.

Eckerstorfer, M. (2013). *Snow avalanches in central Svalbard: A field study of meteorological and topographic triggering factors and geomorphological significance.* Arctic Geology Department, The University Centre in Svalbard, Norway: PhD Thesis.

Eckerstorfer, M., & Christiansen, H. (2011). Topographical and meteorological control on snow avalanching in the Longyearbyen area, central Svalbard 2006-2009. *Geomorphology , 134* (3), pp. 186-196.

Ferguson, S. (1984). *The role of snowpack structure in avalanching.* University of Washington, Seattle, USA: PhD Thesis.

Humlum, O. (2002). Modelling late 20th-century precipitation in Nordenskiold Land, Svalbard, by geomorphic means. *Norsk Geografisk Tidsskrift - Norwegian Journal of Geography , 56* (2), pp. 96-103.

Humlum, O., Christiansen, H., & Juliussen, H. (2007). Avalanche-derived rock glaciers in Svalbard. *Permafrost and Periglacial Processes , 18* (1), pp. 75-88.

Humlum, O., Instanes, A., & Sollid, J. (2003). Permafrost in Svalbard: A review of research history, climatic background and engineering challenges. *Polar Research , 22* (2), pp. 191-215.

Jordan, R. (1995). Effects Of Capillary Discontinuities On Water Flow And Water Retention In Layered Snowcovers. *Defence Science Journal , 45* (2), pp. 79-91.

Jordet, S. (2017). *Validering av Snowpack for norske forhold - Mot en batsnø- og sørpeskredsindeks i Norge?* Department of Geosciences , University of Oslo, Norway: Master Thesis.

Landrø, M., Mikkelsen, O.-A., & Jaedicke, C. (2017). *Gjennomgang og evaluering av skredhendelsen i Longyearbyen 21.02.2017.* Norges Vassdrags- og energidirektorat (NVE).

Lehning, M., Bartelt, P., Brown, B., Russi, T., Stöckli, U., & Zimmerli, M. (1999). SNOWPACK model calculations for avalanche warning based upon a new network of weather and snow stations. *Cold Regions Science and Technology , 30* (1), pp. 145-157.

Major, H., Haremo, P., Dallmann, W., & Andresen, A. (2001). Geological map of Svalbard 1:100000. C9G Adventdalen. Norsk Polarinstitutt.

Marshall, J., & Plumb, R. (2008). *Atmosphere, Ocean and Climate Dynamics: An Introductory Text.* Burlington, Massachusetts, USA: Elsevier Academic Press.

McClung, D., & Schaerer, P. (1993). *The Avalanche Handbook.* Washington, Seattle, USA: Mountaineers.

Met.no. (2017, 11 17). *Meteorologisk Institutt*. Retrieved 5 10, 2018, from About Arome-Arctic: https://www.met.no/en/projects/The-weather-model-AROME-Arctic/about

Met.no. (2018). *Meteorologisk Institutt*. Retrieved 4 18, 2018, from The AROME-Arctic weather model: https://www.met.no/en/projects/The-weather-model-AROME-Arctic

Norgeskart. (2018). *Norgeskart*. Retrieved 6 5, 2018, from Longyearbyen: https://norgeskart.no/#!?project=seeiendom&layers=1002,1015&zoom=10.576666666666664&lat=8681983.78&lon=514503.43&sok=long

Pahaut, E. (1976). *La Métamorhpose Des Cristaux De Neige (Snow Crystal Metamorphosis).* Monographies De La Météorologie Nationale. Météo France.

Rogers, J., Yang, L., & Li, L. (2005). The role of Fram Strait winter cyclones on sea ice flux and on Spitsbergen air temperatures. *Geophysical Research Letters , 32* (6), pp. n/a-n/a.

Saltelli, A. (2017, 3 13). *AndreaSaltelli*. Retrieved 5 10, 2018, from Sensitivity Analysis: http://www.andreasaltelli.eu/file/repository/Bergen_Andrea_Thursday_SA.pdf

Sato, T., Kosugi, K., Mochizuki, S., & Nemoto, M. (2008). Wind Speed Dependences Of Fracture And Accumulation Of Snowflakes On Snow Surface. *Cold Regions Science And Technology , 51* (2), pp. 229-239.

Schaerer, P. (1986). Weather patterns for major avalanches. *The Avalanche Review , 4* (3), p. 2.

Schuler, T., Dunse, T., Østby, T., & Hagen, J. (2013). Meteorological conditions on an Arctic ice cap - 8 years of automatic weather station data from Austfonna, Svalbard. *International Journal of Climatology , 34* (6), pp. 2047-2058.

Schweizer, J., & Wiesinger, T. (2001). Snow Profile Interpretation For Stability Evaluation. *Cold Regions Science And Technology , 33* (2), pp. 179-188.

Strangeways, I. (1985). A cold regions automatic weather station. *Journal of Hydrology , 79* (3), pp. 323-332.

Svendsen, J., & Mangerud, J. (1997). Holocen glacial and climatic variations on Spitsbergen, Svalbard. *The Holocene , 7* (1), pp. 45-57.

Temper, B. (2008). *Staying Alive in Avalanche Terrain.* Seattle, Washington, USA: Mountaineers Books.

Vikhamar-Schuler, D., Müller, K., & Engen-Skaugen, T. (2011). *Snow modeling using SURFEX within the CROCUS snow scheme.* Division for Model and Climate Analysis, R&D Department. Norwegian Meteorological Institue.

Vionnet, V., Brun, E., Morin, S., Boone, A., Faroux, S., Le Moigne, P., et al. (2012). The Detailed Snowpack Scheme Crocus And Its Implementation In Surfex v7.2. *Geoscientific Model Development , 5* (3), pp. 773-791.

Yen, Y. (1981). *Review of Thermal Proporties of Snow, Ice and Sea Ice.* CRREL.

Yr. (2015a, 12 16). *Yr*. (Meteorologisk Institutt) Retrieved 2 12, 2018, from Longyearbyen (Svalbard): Datosøk: https://www.yr.no/sted/Norge/Svalbard/Longyearbyen/almanakk.html?dato=2015-12-16

Yr. (2015b, 12 19). *Yr*. (Meteorologisk Institutt) Retrieved 4 24, 2018, from Longyearbyen (Svalbard): Datosøk: https://www.yr.no/sted/Norge/Svalbard/Longyearbyen/almanakk.html?dato=2015-12-19

Yr. (2015c, 12 18). *Yr*. (Meteorologisk Institutt) Retrieved 2 12, 2018, from Longyearbyen (Svalbard): Datosøk: https://www.yr.no/sted/Norge/Svalbard/Longyearbyen/almanakk.html?dato=2015-12-18

Yr.no. (2018, 5 30). *Yr.no*. (Meteorologisk Intistutt) Retrieved 5 30, 2018, from Weather Statistics for Longyearbyen Svalbard: https://www.yr.no/place/Norway/Svalbard/Longyearbyen/statistics.html